UNIVERSITY OF TROMSØ UIT

Department of Clinical Medicine

Faculty of Health Sciences

Virtual Dissection of Cardiac Motion:

What do we Measure by

Strain and Strain Rate Imaging?

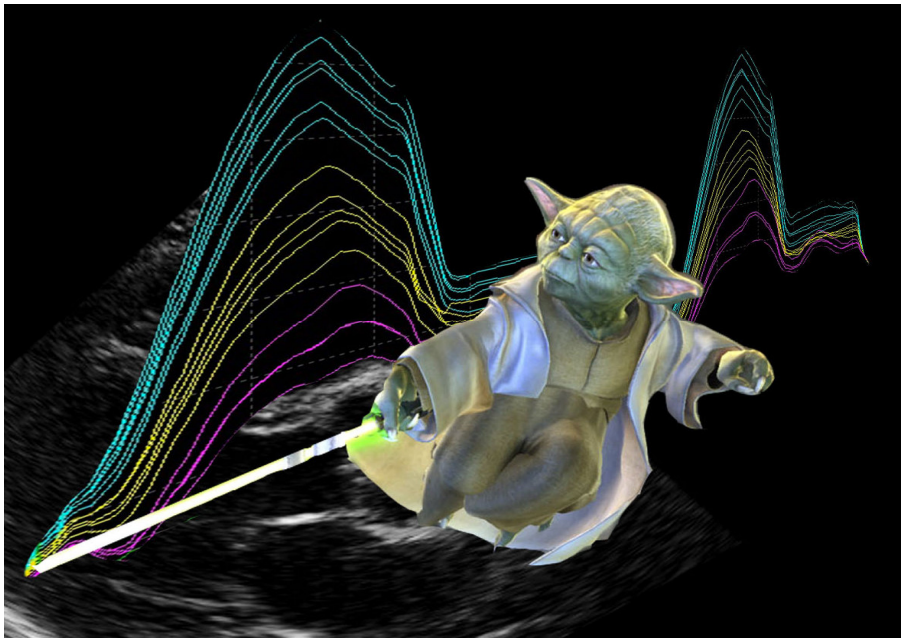

Assami Rösner

A dissertation for the degree of Philosophiae Doctor

September 2010

Im Gedenken an meinen Vater

Acknowledgements

Most of all I want to thank my supervisor *Truls Myrmel* for his attitude saying: "yes" before asking "what was the question?" This attitude was probably the best way to convert my slightly megalomaniac ideas to down to earth results. After one year of high investments like the purchase of an even newer echomachine and three more laborious years to accomplish the clinical study, he did not loose his enthusiasm for my research. *Truls* always gave me his support, and allowed me to develop creative projects. This freedom always motivated me to proceed, even in times when obstacles seemed to be insurmountable.

I also want to thank the research group from the St. George Hospital in London, where I was allowed to stay for two months to get first insights into the field of strain and strain rate imaging. *George Sutherland* has been the most inspiring teacher and lecturer I have ever met. *Bart Bijnens*, the super-brain always had time for interesting discussions. To perform a study about heart size and strain was his idea. However, it was not easy to find an agreement when we tried to explain our findings. The consensus was that heart size and strain were able to increase researchers' blood pressure and heart rate with great effect. I thank also *Aigul Baltabaeva* for supporting this work by spending many hours in the Norwegian embassy, coming to Tromsø and analyzing data for MRI interobserver variabilities. Markus and I tried to express our gratitude by taking her to a boat trip that unfortunately took a dramatic James Bond like ending.

I am very grateful to *Derk Avenarius* who was working with the main amount of work namely all MRI analyses. Luckily, none of us knew in advance, how many hours of analysis the PRODOS study would take. However, the analyses are finished and today we own a capacious database with the potential for numerous future papers. *Siri Malm* has to be thanked for analyzing the interobserver variabilities of the echocardiographic parameters. She has been the most critical co-author and a very valuable partner for discussions and I am hoping for further joint projects. I thank

Amjid Iqbal for reanalyzing all coronary angiograms in the PRODOS study and his friendly and helpful attitude.

Ole Jakob How has been the most important partner in the Animal Research Laboratory to discuss and conduct the pig experiments. He gave me insight into the physiologists` way of thinking that was not easy to understand for a cardiologist. Most importantly, *Ole Jakob* helped me to understand that there were substantial differences between elephants and mice. *Inger Sperstad* has done a great job with creating databases and writing macros for data extraction in all three studies. Without her macros, the data analyses would have become a never-ending story. The help of *Reidun Hansen* was crucial to succeeded in recruiting patients for the PRODOS study. I thank for her continuous intense engagement to find suitable patients and fitting them into the surgical time schedule. *Bente Mathisen* has been helping me a lot with data work and *Tom Wilsgård* gave me support in all simple and sophisticated statistical problems.

I am very grateful for the engagement in the PRODOS study of the clinical research unit under the leadership of *Elin Evensen* and *Anne-Sofie Sand*. *Annika Gustafsson* was a fantastic initiator who arranged all logistics and gave the study a smooth start. *Britt-Ann Winther Eilertsen* overtook the relay and was steering the logistics perfectly until the end of the study. V*igdis Moe*, *Stein-Gjøran Birkeland, Trond Isaksen* and *Elin Hansen* all learned to assist the dobutamine stress echo test and were great help in accomplishing the study. All of them created a positive atmosphere for the patients who obviously were looking forward to meeting us again.

Further, I have to thank the staffs from the MRI department who were crucial for realizing PRODOS. *Peggy Larsen* was the main coordinator for MRI examinations. *Bente Kristiansen* traveled to Berlin learning all necessary expertise for cardiac MRI acquisitions in ischemic heart disease. *Arild Gjerdrum, Tone Ann Andreasen* and *Vibeche Gabrielsen* overtook MRI in the PRODOS study and together with *Derk* and *Bente* helped to establish a team for cardiac MRI in Tromsø. *Gunnar Arveschoug* has to be thanked for excellent service, he was helping out

immediately when problems with the echomachine or software arose. I want to thank *Birgit Bohn* for much more than for providing me the speckle tracking software. Furthermore, I am also very grateful to all the patients participating in the study, who underwent a very laborious study protocol.

Many thanks to *Arthur Revhaug* and *Terje Larsen* who provided the facilities of the Surgical and Physiological Animal Research Lab and to everyone who helped me to conduct the pig experiments. *Erling Aarsæther, Stig Müller, Thor Alan Stenberg* and *Magna Hansen* were essential help for the instrumentation. *Knut Steinnes, Frederik Bergheim* and *Harry Jensen* supported me with their technical expertise and their brilliant ideas. The foot pedal on the respirator will change life for all future researchers and technicians in the pig lab. Thanks for the technical assistance and for always creating a cheerful atmosphere in the lab (also handling perfectly the swinging moods of pregnant women) to *Hege Hagerup, Viktoria Steinsund, Janne Andreassen, Christine Young, Jenny Ratree Duangthang, Monica M. Figenschau, Kine-Mari Hanssen, Mehrdad Sobhkhez* and *Trine Kalstad. Thomas Andreasen* and *Timofei Kondratiev* helped me to analyze tissue flow with microspheres.

I am deeply grateful to *Per Lunde* my inspiring mentor in the field of echocardiography. He opened me new dimensions in the world of echocardiography and always had time for the most exciting discussions.

I further have to thank my former and current chiefs of the Cardiological Department, *Knut Rasmussen, Einar Bugge* and *Pål Tande* for giving me the possibility to combine research activities with interesting clinical work. *Knut Rasmussen* bears the burden of being responsible for blindly having employed me before he ever saw me in Tromsø. Thus, a long story began that comprised much more than only this work.

All my friends have to be thanked for every single moment they shared with me. Every moment had its special importance. I thank *Bärbel Irion* for having been the most important support in most difficult times. Further, I thank *my mother* for coming to Tromsø and being a caring grandmother.

Finally, I thank you, *Markus* and *Nico* for being the heart of my life. What you mean to me cannot be expressed in words.

Contents

1 List of Papers

Paper I

Left ventricular size determines tissue Doppler derived longitudinal strain and strain rate

Assami Rösner, MD; Bart Bijnens PhD, Magna Hansen MD, Ole Jakob How PhD, Erling Aarsæther MD; Stig Müller,MD, PhD; George R. Sutherland, MD, FESC and Truls Myrmel, MD, PhD European Journal of Echocardiography (2009) 10, 271–277

Paper II

High resolution speckle tracking dobutamine stress echocardiography reveals heterogeneous responses in different myocardial layers: implication for viability assessments

Assami Rösner, MD; Ole Jakob How, PhD; Erling Aarsæther, MD; Thor Allan Stenberg; Thomas Andreasen; Timofei V. Kondratiev, MD, PhD; Terje S. Larsen, PhD and Truls Myrmel, MD, PhD, Journal of the American Society of Echocardiogrphy (2010) in print

Paper III

Longitudinal strain in patients with coronary artery disease and preserved ejection fraction. Implications for dobutamine stress echocardiography and tissue Doppler derived strain and strain rate

Assami Rösner, MD; Derk Avenarius, MD; Siri Malm, MD, PhD; Aigul Baltabaeva, MD, PhD; Amjid Iqbal, MD, PhD; George R. Sutherland, MD, FESC; Bart Bijnens, PhD; Truls Myrmel, MD, PhD, submitted

2 Selected Abbreviations

BMI	Body mass index
BP_{sys}	Systolic blood pressure
BSA	Body surface area
CABG	Coronary artery bypass graft
CAD	Coronary artery disease
CO	Cardiac output
DSE	Dobutamine stress echocardiography
EDV	End diastolic volume
EF	Ejection fraction
ET	Ejection time
HR	Heart rate
LAD	Left anterior descending (coronary artery)
LE	Late enhancement (gadolinium contrast)
LV	Left ventricle/left ventricular
MAP	Mean arterial pressure
MRI	Magnetic resonance imaging
PET	Positron emission tomography
PSI	Post systolic index
PSS	Post systolic strain
ROI	Region of interest
SPECT	Single photon emission tomography
SR	Strain rate
SRI	Strain rate imaging
SV	Stroke volume
TDI	Tissue Doppler imaging
WMS	Wall motion score

3 Introduction

Noninvasive evaluation of regional myocardial function has rising diagnostic value in several myocardial disorders. Especially in coronary artery disease, the evaluation of regional myocardial function is of importance to accurately assess the degree and location of viable and ischemic tissue[11, 12].

There exist numerous imaging techniques for non-invasive assessment of viability i.e cine magnetic resonance imaging (MRI), MRI-tagging, late enhancement (LE)-MRI, gated blood pool scanning (GBPS), single photon emission tomography (SPECT), positron emission tomography (PET) and echocardiography with dobutamine stress (DSE). Among all these techniques, DSE is most widely used due to its highest availability and relatively low cost[113]. Traditionally DSE is used in combination with assessment of wall motion score (WMS), using qualitative visual interpretation of two-dimensional (2D) imaging loops. Even though WMS-assessment in DSE has higher specificities for viability assessment compared to other classical methods like SPECT and PET[11, 12], the high inter-observer variability and dependency on observer-experience hamper the interpretation of individual tests[59]. Thus, the need for quantification and high temporal resolution for a more accurate assessment of regional myocardial function became obvious.

Since Isaaz published a report on tissue velocity imaging in 1989[63], there has been started an enormous development on ultrasound based imaging of regional myocardial motion. Several studies have confirmed the accuracy of the method in experimental and clinical settings[35, 48]. The first approach using velocity based strain and strain rate (SR) imaging came from Trondheim, Norway, reported by Heimdal et al. in 1998[54]. Consecutive in vitro phantom studies and experimental studies subsequently have validated these tissue Doppler imaging (TDI) based strain and SR measurements and verified their reproducibility[42, 91, 129]. A series of experimental and clinical studies have

confirmed the accuracy of the strain rate imaging (SRI) in reflecting different contractile states and differing ischemic substrates [35, 39, 118, 134].

Additionally, 2 dimensional (2D) strain imaging was developed [18, 81] and implemented in commercially available software. By using speckle tracking in 2D grey scale imaging, the angle dependency of TDI strain was almost overcome, allowing assessment of circulatory, longitudinal and radial strain as well as the quantification of myocardial twisting. This method has been evaluated experimentally and clinically and tested against TDI strain and MRI tagging[3, 4, 68]. Several studies have confirmed the value of using SRI either by TDI[52, 62, 117, 118, 134] or 2D strain [26] in assessing viability, grading and location of ischemic lesions.

However, strain and SR do not measure myocardial contractility directly. Strain and SR measure deformation. Thus, experimental studies already showed that strain and SR depend on the interaction of contractile force, extrinsic loading conditions, ventricular geometry and the elastic properties of the tissue[1, 15, 119, 120, 129, 134].

4 Aim of the thesis

1. To investigate various factors influencing strain and SR measurements in particular the influence of ventricular size, loading conditions and the influence of heterogeneously deforming myocardial layers.

2. To explore the correlation of strain and tissue flow in different myocardial layers using an experimental set-up with a high grade-coronary stenosis and during dobutamine stress.

3. Finally to investigate in a clinical study whether TDI SRI could quantify myocardial segmental dysfunction in coronary artery disease (CAD) and predict functional improvement after coronary artery bypass grafting (CABG).

5 Background

5.1 Strain and SR Imaging

The non-invasive assessment of regional myocardial function using a clinical bedside test is of major interest to the clinician. However, the non-invasive measurement of myocardial contractility is not straight forward[72]. When defining myocardial function as the ability of the cardiac muscle to develop force at constant loading conditions and heart rate (HR)[96], regional force development in the intact heart cannot be measured directly like in a muscle strip experiment. According to Newton's law, force results in acceleration of a body. Therefore, motion and deformation of the myocardial muscle indirectly reflect contractile force; given that loading conditions, tissue elasticity and HR can be accounted for.

Myocardial tissue velocities have the potential to give information about cardiac motion. However, by definition, tissue velocities in longitudinal direction increase with the length distance from the probe. This results from the dependency of velocities from the amount of myocardial tissue deforming between the probe and the region where the Doppler measurements are obtained. Thus, basal longitudinal velocities express the sum of motion in apical, mid and basal segments in addition to motion of the heart in the thorax. Strain and SR measurements have been developed with the intention to measure "true" regional deformation, overcoming the problem of tethering and total heart motion[117]. Implementing strain-measurements by TDI and 2D strain in echocardiography opens for quantification of cardiac deformation at high temporal resolution in nearly all segments of the left ventricle.

In physics, strain is the geometrical measure of deformation of an elastic body. In cardiac imaging, strain is being used in a simplified manner as linear strain, where one-dimensional linear strain can be defined by the Lagrangian formula:

$$\varepsilon = L - L_0/L_0 = \Delta L/L_0$$

where ε is strain, L_0 is the initial length of a body, L is the instantaneous length at the time of measurement. Strain is expressed as the percentage of initial length, being negative at shortening and positive at lengthening or stretching compared to the initial length.

Figure 1: The three dimensions of linear strain in the heart

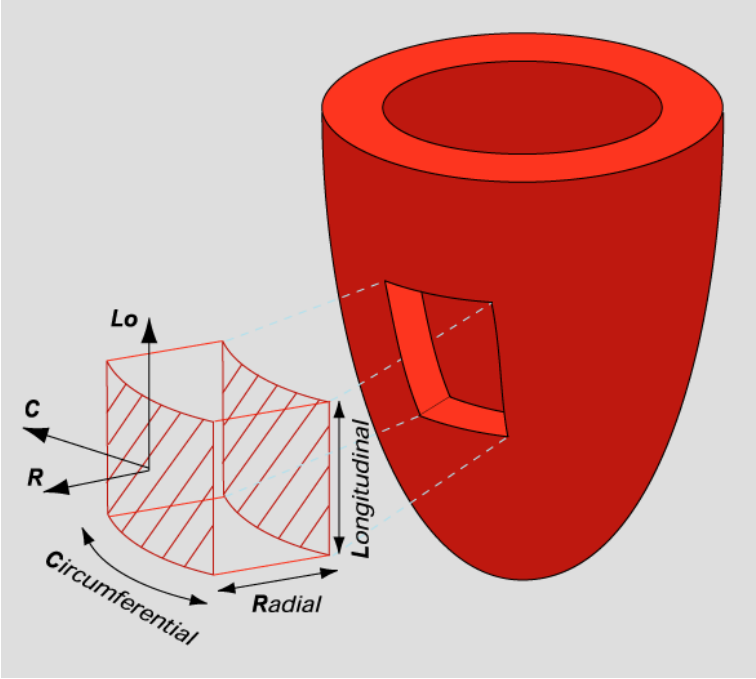

J. D'Hoodge et al. Eur J Echocardiography (2000)

The deformation of the myocardium can be described in three dimensions as three linear strains and six shear strains as angular distortions. In cardiac physiology the three linear strain dimensions are defined in relation to the heart axes as longitudinal and circumferential shortening and as radial thickening[90] as depicted in figure 1.

Strain rate (SR) is the instantaneous strain (or change in strain) per time unit:

$$\dot{\varepsilon} = \Delta\varepsilon / \Delta t$$

where $\dot{\varepsilon}$ is SR, and t is time. The unit of SR is s^{-1}. Strain is also the time-integral of SR. Figure 2 illustrates velocities and displacements compared to strain and SR in the same heart.

Figure 2 Velocity and displacement are dependent on the position in the myocardium, whereas strain and SR are not

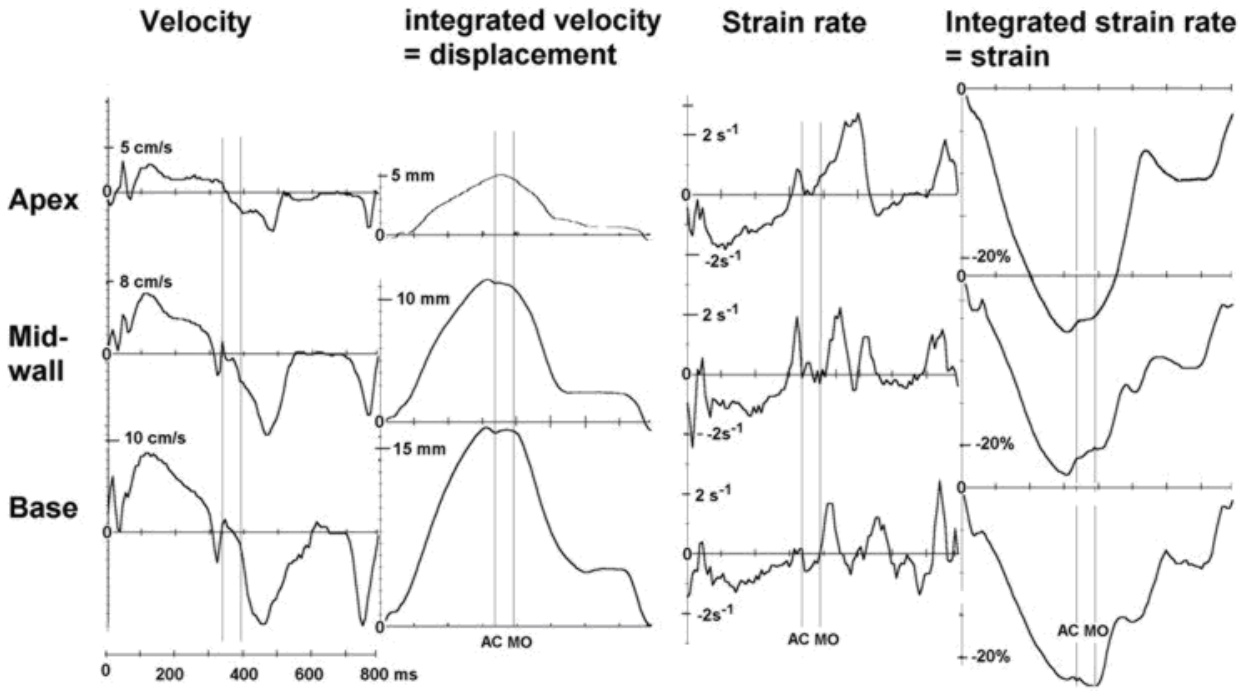

Støylen: http://folk.ntnu.no/stoylen/strainrate

5.2 Effect of Loading on Strain and SR (Paper I)

Strain or SR can be related to contractility and are clinically used as indicators to assess contractility in myocardial disease. However, from experimental muscle stripe and animal studies it is known, that strain must be dependent on the interaction between contractile force, extrinsic loading conditions, ventricular geometry and the elastic properties of the myocardium[107]. Preload or presystolic fiber stretch in the intact heart is influenced by ventricular diastolic filling pressure, venous return, atrial function, cardiac shunts or valvular leakage. Afterload or systolic wall stress is

dependent on arterial impedance, valvular function, wall thickness and ventricular geometry. Several physiological studies describe the dependency of wall thickening or muscle fiber strain on loading[1, 23, 34]. Increased muscle strain in the heart due to increased preload and initial fiber stretch can usually be elicited by a short-term end diastolic volume overload. Increase in afterload or systolic wall stress decrease the amount of deformation[1]. However, the physiological experiments have been based on either isolated hearts, muscle stripe experiments or open chest models. SR in response to loading has not been equally extensively investigated[1, 119, 120, 129]. But an experimental open chest model indicated also the dependency of SR on loading[129]. The HR is not known to influence strain and SR parameters directly[15] but may have an influence on loading when ventricular filling is impaired due to extensive shortening of the diastole. Furthermore, in ischemic heart disease, high heart rates might decrease diastolic coronary blood flow substantially, thus decreasing strain by decrements in contractile force[134].

5.3 Strain and Heart or Body Size (Paper I)

Population studies on either gender have shown varying strain values with decreasing strain towards increasing body mass[55]. A study investigating normal strain and SR values in children found longitudinal strain changing dependent of age. The interpretation of this observation was somewhat difficult, since HR seemed to have a parallel impact on strain values[15]. Whether body size, gender, obesity or age are independent factors, influencing strain remains unclear. A mathematical model showed that bigger hearts at unchanged contractile force ejected the same amount of stroke volume (SV) at lower strains and SR than smaller hearts[82].

Figure 3. *Mathematical model showing dependency of contractility, strain, SR on end diastolic volume and stroke volume*

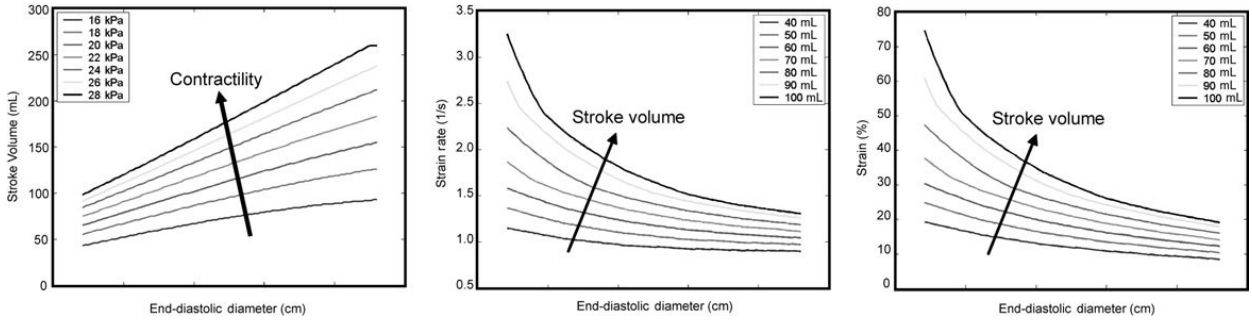

Marciniak A et al. Eur Heart J 2005

However, in healthy individuals of varying body and heart sizes, one would expect bigger hearts to maintain ejection fraction (EF), eject a relatively higher SV and therefore have the same strain-values compared to smaller hearts. Investigating adult dogs with large variation in sizes Nakano et al. did not find differences in stress strain relation according to heart/body-size[94]

5.4 Myofiber Architecture in the Left Ventricle (Paper II)

Regional myocardial deformation is dependent on myofiber-orientation. Spiral myofiber architecture and the helical arrangement of myofibers in the left ventricle build a complex system that might explain differing motion patterns from layer to layer. Anatomical and histological studies have shown myofiber loops descending clockwise from the base to the apex and ascend counter clockwise[49]. Fiber direction is predominantly longitudinal in the subendocardial and subepicardial region whereas the main direction of fibers in the middle part is circumferential[49]. The epicardial and endocardial fibers of the ventricular wall are made of myocytes orientated with the angles of their long axes almost at 90 degrees to each other[49].

Figure 4 Myofiber-orientation in different myocardial layers

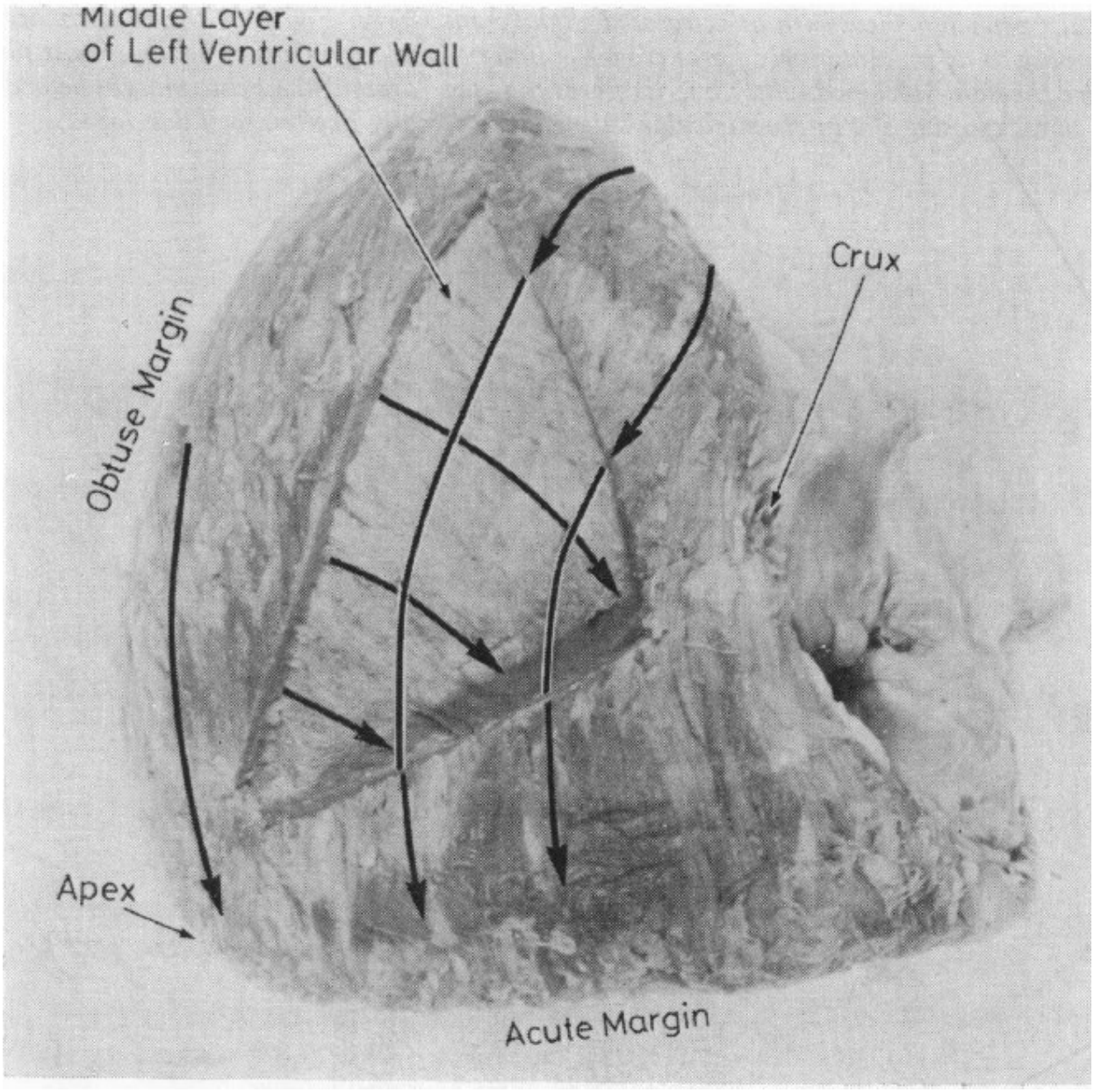

Greenbaum Br. Heart J 1981

Myocytes are organized into sheets that are stacked shingle-like, transducing a 14% decrease in myocyte length to 40% thickening of the left ventricular (LV) wall by increasing sheet angles during systole[28, 30]. Following the main fiber direction with differently curved knifes reveals that myofiber sheets are not aligned completely parallel to one another, rather the myofiber sheets

diverge within the LV wall creating angulations with respect to the plane of the epicardial surface [80]. The complex left ventricular architecture with anisotropy of fiber orientation and differing fiber angles inside the myocardial layers gives reason to the assumption of varying regional motion in layers of myocardial segments at different locations of the left ventricle.

5.5 Resting Layer-Strain Heterogeneity (Paper II)

One, two and three- dimensional functional analyses of different myocardial layers have been performed with different methods. The highest spatial resolution can be achieved with transmural radio-opaque bead markers under biplane cineradiography. This method allows three dimensional analysis of normal fiber and sheer strains[6, 76, 105]. It has been shown that non parallel plane orientation and consecutive intramyocardial sheer strains contribute most to myocardial wall thickening. Also with transmural sonomicrometry crystals, the main tracking direction along the subendocardial and subepicardial segments could be demonstrated[110, 111]. The late mechanical activation of the subepicardial layers leads to an initial stretch in the isovolumic contraction period while the subendocardial layers already contract[110]. In several studies, subendocardial radial strains have been shown to be higher than subepicardial strains[36, 92]. Radio-opaque beads give important physiologic and pathophysiologic information and have been used in animal studies and in posttransplant patients [38, 50, 87, 89, 138]. However, the method is limited to experimental open-chest-settings and has technical limitations by inducing injuries to the region of interest (ROI).

Non-invasive methods have demonstrated similar effects indicating inhomogeneity of ejection time (ET)-strain in different layers[17, 53, 85, 86, 93, 100]. 2D strain allows interpretation of deformation in 3 dimensions on 2 perpendicular imaging loops. In contrast to TDI derived values and radioopaque markers it is possible to measure strains in the most outer and inner myocardial wall regions with this method.

Using a high resolution 5-12 MHz probe allows high spatial resolution without reduction of temporal resolution. Thus, the use of high resolution 2D strain opens for “non invasive” assessment of layer strains in different experimental condition in an open thorax model.

5.6 Myocardial Deformation in Varying Ischemic Substrates (Paper II + III)

Several studies using different methods for the assessment of regional wall motion have shown that flow reduction, acute ischemia, subendocardial infarctions and transmural infarctions lead to a gradual decrease in strain and SR and that the value of measured strain and SR is a potent tool to detect different ischemic substrates[15].

In early experimental studies, ultrasonic crystals were implanted to assess changes during acute ischemia. It has been shown that acute ischemia causes acute decrease in myocardial radial and longitudinal strain. Additionally, the magnitude of these changes is proportional to the severity of the acute ischemic insult or the amount of flow reduction[21, 32, 57, 61, 78, 124, 126, 127].

Combined measurements of deformation and blood flow in different myocardial layers have shown a linear relation between flow reduction and radial deformation. Flow reductions mainly restrict subendocardial tissue flow and strains, while subepicardial flow and strains stayed normal despite excessive coronary constrictions[43-45, 51, 130]. Thus, as demonstrated in an experimental study, endocardial fiber shortening decreased within 5 seconds of the onset of ischemia, whereas epicardial fiber shortening was not affected until 30 seconds of ischemia[101]. During ischemia, endocardial segment-length shortening was reduced more than epicardial shortening as a result of decreased blood flow and altered metabolism in the endocardium[7]. Wang et al. used intracardial high resolution ultrasound to measure DTI and M-mode derived radial strains[132]. In accordance with

earlier experimental studies, they demonstrated a gradual decrease of endocardial to epicardial strain in increasing ischemia.

In addition to transmural radial strain gradients at rest and during ischemia, some studies imply changes in longitudinal or circumferential strain gradients during acute ischemia[44, 76, 105]. Thus, regional deformation studies with radio-opaque markers investigated strain changes after short coronary artery occlusions and showed marked decrease in fiber strain and circumferential strain, whereas radial and longitudinal strain was not significantly changed[76]. Non-invasive studies on layer strains during ischemia have so far mainly been describing one-dimensional, mainly radial deformation, whereas high resolution epicardial 2D strain opens for layer-strain assessment in three dimensions during different interventions.

5.7 Dobutamine Stress Echocardiography with Strain Imaging (Paper II + III)

Dobutamine stress is widely used as a clinical bedside test to identify inducible ischemia and viable myocardium. The method employs the principle that stunned myocardium and myocardium with flow reserve will respond to inotropes (dobutamine stimulation)[65]. Dobutamine stimulation thus reveals viable myocardium despite reduced function at rest. In contrast, to viable myocardium, transmural infarctions do not respond to dobutamine. In DSE, akinesia at rest and missing dobutamine response is being used as an indicator for transmural scars and thus no functional recovery after revascularization[125]. An experimental study investigating M-mode and TDI derived radial strain and SR with controlled blood flow reduction and with dobutamine stress showed the correlation of gradual decrease in radial endsystolic strain values and blood flow reduction and no dobutamine response in the absence of coronary flow reserve[64].

Thus, the quantification of deformation seems to be important for the diagnostic value of a dobutamine-stress test. Several studies have shown clinical usefulness of accomplishing DSE by

SRI[14, 26, 52, 60, 131, 135, 137]. However it is still unclear if the DSE response is equal in longitudinal, radial or circumferential direction. Hanekom et al. showed that longitudinal strain rate imaging was more sensitive to detect viability than (radial) wall motion scoring[52]. A study of Zhang et al. found that longitudinal SR could differentiate transmural, subendocardial infarctions and normal myocardium[142]. Chan et al. demonstrated that longitudinal strain and SR are already decreased in subendocardial infarctions, whereas circulatory strain and SR stay normal until the infarct size exceeds 50% of wall thickness[26]. These studies indicate that longitudinal strain possibly is more sensitive to ischemic lesions in the subendocardium, whereas radial and circumferential strains are more sensitive to predict normalization in viable myocardium. To my knowledge, the effect of dobutamine stress on ischemic tissue has neither been studied using three dimensions of strain and not on different myocardial layers. Furthermore it is still unknown, whether subendocardial or mid-\myocardial layers have the potential to be activated by dobutamine. If so, the transmural extend of infarctions could be defined by quantification of layer-strains during DSE.

5.8 Viability and Hibernation (Paper III)

Common causes of ischemic left ventricular (LV)-dysfunction are transmural myocardial infarctions, subendocardial infarctions, myocardial stunning and myocardial hibernation/ repetitive stunning. These states are difficult to differentiate, and complicated by the potential coexistence of different states in the same myocardial region. The term “viable myocardium” or viability is often used to describe mechanically dysfunctional myocardium still being vital. Different tests for viability like PET, SPECT, LE MRI, enddiastolic wall thickness or functional tests like dobutamine stress test also define “viable” differently using nuclear function, metabolic function, membrane function, the absence of myocardial scar tissue or contractile reserve[128]. Late enhancement MRI is in many aspects the clinical gold-standard in assessing myocardial viability[21-23]. With this technique

gadolinium-chelate (Gd) is infused, and late enhancement (LE-MRI) demonstrates both interstitial and replacement fibrosis. However, whether applied to a myocyte or to a segment of myocardium, this description of viability implies nothing with regard to recovery of the contractile state.

In contrast to viability, *hibernation* is defined as the state of contractile dysfunction in the setting of chronic ischemic heart disease[103]. Hibernating myocardium is by definition viable but dysfunctional myocardium that improves in function after revascularization. This definition, of course, assumes that revascularization is successful and that the procedure itself does not lead to damage of the relevant area of myocardium[128]. Many aspects remain unclear around the term *hibernation*. It is varying to what extent the perfusion is reduced at rest. In addition, repeated ischemic attacks can result in chronic dysfunction, with resting flow remaining normal, a condition also termed *repetitive stunning*. In the clinical setting different situations may co-exist from normal to reduced flow at rest and different degrees of reduced flow reserve.

Animal models of chronic myocardial hibernation are rare. Biopsies taken from areas of viable but dysfunctional myocardium at the time of coronary bypass grafting in patients have shown quite severe changes of the cardiomyocytes themselves and in the extracellular matrix. There is a variety of cellular and subcellular degeneration with varying degrees of degeneration and fibrosis[56]. The likelihood of recovery of function after revascularization is related to the extent of myocyte injury, apoptosis and amount of replacement fibrosis[112]. The early changes may be reversible before significant structural disorders occur, but the loss of myocytes is obviously not reversible. Thus, long-term hibernation may lead to irreversible loss of myocardial function[128].

6 Methods and Methodological Considerations

6.1 Experimental Setting (Paper I + II)

Animal experiments were conducted in accordance with the Guide for the Care and Use of Laboratory Animals published by the National Institutes of Health (Publication No 85-23). Experimental protocols for handling and sedation of the pigs were all approved by the local committee of the Norwegian Experimental Animal Board. Experimental studies were performed with domestic pigs (cross-breeds of Norwegian Landrace and Yorkshire) of both sexes weighing 12.5-70 kg in paper I and 37.7 ± 2.4 kg in paper II. The pigs were provided by one local breeder and housed at the animal department. The premedication anesthesia, continuous fluid- infusions and instrumentation followed a standard protocol used in our laboratory like described in paper I and II.

6.2 Patient Selection (Paper III)

Patients in paper III were selected from all patients referred to the cardiothoracic surgical department UNN for a CABG operation. From several patients meeting inclusion criteria (in general two to five) only two patients per week could be selected due to limited MRI capacity. Our aim was to analyze a wide range of ischemic substrates. Thus, we tried to select at least one third of patients with previous myocardial infarctions in order to analyze a significant number of segments with positive LE-MRI. Power-calculations assuming a 10% difference in strain-values at a type II error limit of 5% indicated that 60 patients were needed in the study. Because of early dropouts, the number was extended to 67 patients. However, only three women could be recruited to the study, and the ratio between sexes does therefore not represent the average population of CABG patients. The low number of female participants was due to the fact that women undergoing a CABG operation are 10 years older than the male CABG patients and thus more unwilling to submit to the

extra stress of being a study participant. In addition, many of the female CABG patients in our study population met exclusion criteria due to a high percentage of atrial fibrillation and additional comorbidities. Lastly, the CABG–patients with previous infarctions were also predominantly men.

6.3 Fluorescent Microspheres (Paper II)

The use of colored microspheres has been established as a standard procedure for tissue flow measurements[73]. In this method, a defined number of microspheres is injected into the left atrium and subsequently distributed in different organs according to the regional tissue flow. Microspheres at a diameter of 15µm cannot pass the capillary bed. Thus, the microspheres are caught in the peripheral vascular bed during the first perfusion after their infusion. The number of microspheres applied, should be high enough to reach a minimum number (approximately 400 microspheres) per excised tissue piece in order to gain reliable results by photometry. On the other hand, too high concentrations of microspheres in the tissue may cause embolization and reduce the tissue flow. A microsphere concentration of 400 to 1500/g tissue was proven to be ideal. At various stages of the experiment, microspheres of different colors were injected into the cavity of the left atrium. The tissue at final analysis thus contains several numbers of microspheres where each color represents the flow at the different experimental stages. At the time of analysis, the excised tissue is resolved and the color concentration measured by photometry. A set of five fluorescent colors was used in the study. Spectral overlap was insignificant. A reference sample was taken from the femoral artery at a defined flow velocity (here 4.12 $ml \cdot min^{-1}$) at a defined time-period after injections, namely 2 minutes. Tissue flow can be calculated by the following formula:

$$\text{flow}_{\text{tissue}} = \text{flow}_{\text{reference}} * \text{microspheres}_{\text{tissue}} / \text{microspheres}_{\text{reference}}$$

The result have to be corrected for the sample weight and expressed as tissue flow in $ml \cdot min^{-1} g^{-1}$.

6.4 Myocardial Late Enhancement MRI (Paper III)

LE MRI was used in paper III. The use of the method is based on the principle that myocardial late enhancement in gadolinium-contrast-enhanced cardiac MRI has the ability to delineate precisely myocardial scar associated with coronary artery disease. Gadolinium is a paramagnetic lanthanide- element. It changes signal intensities in MRI by strongly decreasing the T1 relaxation times of the tissues in its surroundings. Infarcts enhance 10-15 minutes after the administration of intravenous gadolinium contrast application. This enhancement represents the accumulation of gadolinium in the extracellular space, due to the loss of membrane integrity in the infarcted tissue[77]. In the clinical study, all acquired images were guided by ECG triggering during one breath-hold. Images were taken from the left ventricular (LV) outflow tract, 4-chamber view and several short axes. In paper III, it was important to define the same segments by echocardiography and MRI. The right ventricle was used to define the position of the septum in short axis views. Imaging of the 3-chamber (view of the left ventricular outflow tract, LVOT) and 4-chamber views were defined in both methods by depicting the same guidance- structures in both methods. However, misalignment of some segments by either method could not be completely excluded as an error source.

6.5 Experimental Echocardiography in Paper I

Paper I was conducted in a closed chest pig model with echocardiography performed in a transthoracal short axis view for registration of radial strain. In pigs apex of the heart points towards the sternum. Thus, the common long-axis imaging with an apical approach cannot be performed. As we intended to investigate mainly changes of longitudinal strain with TDI, we had to alter the

method for an apical approach. By opening the abdomen directly under the xyphoid, but neither opening the intrathoracic cavity nor the peritoneum, an apical subdiaphragmal approach was feasible with additional high image quality. As shown in figure 1 of paper I, a perpendicular imaging aligned with the lateral wall could be recorded. A transesophageal probe (5-MHz) was used for the transdiaphragmal imaging, whereas transthoracal imaging was performed with a S5-1 probe (1-5 Mhz) and an iE 33Ultrasound scanner (Philips Medical Systems, Andover, MA). The higher spatial resolution of the transdiaphragmal imaging might explain the higher quality of longitudinal SRI. Radial ET-strain had much higher variances than longitudinal ET-strain. Therefore, radial strain and SR were not included in analyses of heart size and strain.

6.6 Experimental Echocardiography in Paper II

In paper II, echocardiography was performed in an open chest pig model. A 5 – 12 MHz epicardial probe and the Philips iE33 ultrasound scanner were used. The probe was placed manually on the epicardium, after opening the pericardium. A jelly pad of 0.5 cm was fixed to the probe in order to avoid near-field artifacts. By fixation of the apex with the apical pericardium intact, motion artifacts could be avoided. Recording at the highest dobutamine doses was complicated by the fact that the imaging angle was narrowed at end-systole due to a more rounded epicardial surface leaving small air-filled spaces at the edges of the probe. This occurred especially in the lateral non-ischemic wall. Interestingly, the mid-cardiac twisting seemed to be reduced at higher dobutamine-levels, resulting in lower displacement of all points in circulatory direction and thus allowing reasonable data from a narrowed imaging angle. The total insonation depth was not more than 2 cm; allowing acquisitions at high ultrasound-frequencies. Spatial resolution was not reduced in order to gain higher frame-rates. FRs of 115/min were sufficient to extract peak systolic values without “blunting” of the curves during ET. By this ultrasound method, the imaging of the anterior and

lateral wall was nearly free of artifacts even though the positioning of the stalked probe in the lateral wall was challenging.

6.7 Dobutamine Stress Doses (Paper II + III)

Compared to standard dobutamine-stress-echocardiography protocols[84], very low doses were chosen in paper II and III. Firstly, the dose-response in adolescent pigs had to be tested. Secondly, we observed that doses lower than 10 µg $kg^{-1}min^{-1}$ of dobutamine could increase contractility during reduced resting flow, whereas 10 µg $kg^{-1}min^{-1}$ might already lead to perfusion contraction mismatches with decreased strains. In a pilot study with 4 pigs we tested hemodynamic changes and strain changes at dobutamine doses of 0.1; 0.25 ; 0.5; 1.0;1.5; 2.0; 2.5 ; 5 and 10 µg $kg^{-1}min^{-1}$ were tested. The first observation of increasing strain could be registered at 0.1 µg$kg^{-1}min^{-1}$, increasing again at 0.25 µg $kg^{-1}min^{-1.}$ The next dose-level with an observed increase in strain was 2.5 µg $kg^{-1}min^{-1}$. Based on these observations we chose dobutamine increments of 0.1; 0.25; 2.5; 5 and 10 µg$kg^{-1}min^{-1}$ were chosen in the pig-study and 2.5; 5; 10; 20 µg$kg^{-1}min^{-1}$ for the clinical stress tests.

6.8 Tissue Doppler Imaging Strain

In TDI velocities are derived from 2D color Doppler imaging with mean velocity values calculated for each imaging point. Furthermore, SR is derived from the velocity gradient at two different regions in the myocardium and expresses the length change over time between two measuring points.

$$SR = v_1 - v_2 / l_{1-2}$$

where v_1 and v_2 are the velocities measured at two points and l is the distance between the two points. Strain in TDI is the time integral of SR and in the software QLab (Philips) calculated as

Lagrangian strain. In QLab, a manually placed line (M-line) defines the region of interest (ROI). The M-line angle is defined by the investigator and therefore not necessarily aligned to the ultrasound-beam. In QLab SR is calculated as follows:

$$SR = \frac{v_1 - v_2}{r}$$

where v_1 and v_2 are the velocity magnitudes and r the distance between two measuring points. Because of Doppler angle dependence only the components of $|\vec{v}_1|$ and $|\vec{v}_2|$ along the ultrasound beams can be measured with TDI. The strain rate estimated in QLab, called SR_{QLAB} is defined by the following equation:

$$SR = \frac{v_1 - v_2}{\mathrm{r}} = \frac{|\vec{v}_1| - |\vec{v}_2|}{r \times \cos(\alpha)}$$

Additionally, SR is not calculated as a single measurement between two points with two velocities. It is rather derived from all velocities (and distances) measured along the M-line. Several problems arise with high angle deviations that cannot be overcome by angle-correction: High angle deviations cause increasing variations of velocities, i.e noise, especially when measured in several ultrasound beams. Furthermore, velocities are still not being measured along the M-line, but along the ultrasound beam, leading to measuring radial velocity components instead of longitudinal ones. Therefore, we tried to avoid high angle deviations when using TDI strains. Because of noisier data when applying a curved M-line, we decided to choose three straight M-lines with the maximal length of 1.8 cm in one myocardial wall.

.

6.9 2D Strain

With TDI, only longitudinal strain can be measured in nearly all segments of the left ventricle. But by solving the problem of angle dependency, radial and circumferential strain can be depicted in all segments of the left ventricle. 2D speckle tracking is one approach to measure strain from 2D

imaging loops. The origin of speckle in ultrasonic images is the interference of wavelets reflected by individual scatterers. The resulting interference pattern is closely related to the exact position of the individual scatterers. Small changes of position of scatterers can lead to high differences in interference pattern, creating a "fingerprint" pattern, the speckle. When scatterers translate relative to the transducer but keep their relative positions, the interference pattern will not change. Thus, the speckles will not change their pattern, only their position within the image[81, 123]. If a region is defined in one frame, a search algorithm will be able to recognize the area with the most similar speckle pattern in the next frame within a defined search area[18]. Increasing spatial resolution and number of speckles increase the accuracy of the method[3].

Figure 5 A pattern of speckles are recognized and localized from frame to frame

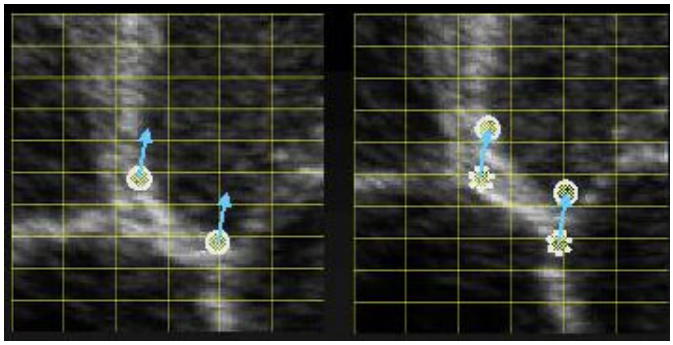

Syngo Velocity Vector Imaging (VVI) Siemens Medical Systems, Erlangen, Germany

In 2D measurements strain is calculated in most systems as Lagrangian strain (by defining an initial length of the tissue at end-diastole) directly derived from two points and the initial length and instantaneous length-change between two points. SR from 2D speckle tracking is being calculated as instantaneous strain-change per second.

6.10 Artifacts in TDI strain (Paper I + III)

TDI derived SR comprises a number of potential artifacts that have been extensively studied and described since the method was introduced[116]. In the present studies, aliasing at resting

conditions was avoided by optimizing Doppler velocities. On the other hand, too high velocities potentially lead to loss of low velocity data. Therefore, the optimal velocity-range must selected for each stage of DSE. Aliasing in the clinical DSE sometimes occurred in basal segments, when the aliasing-velocity was not sufficiently increased during the stress test.

Reverberations are the most important reason for artifacts, arising from stationary structures[116], causing the ultrasound wave bouncing back and forth, prolonging the time traveling through the tissue and therefore projecting the signal to a deeper structure. Thus, reverberations could be avoided in the experimental studies, but were the main cause for discarding measurements in the clinical study. The M-line in QLab could display strain and SR of up to eight subsegments along the M-line. One subsegments had a minimum length of 2 mm. Visualizing these subgroups aided the detection of reverberations in one cardiac cycle, when neighboring subsegments showed inverted strain curves. When strains in various subsegments were homogeneous, good quality of the analysis was ensured.

Near field artifacts constituted a problem in subdiaphragmal echocardiography on pigs but could be avoided by applying a jelly pad to the ultrasound probe. By choosing wall-by-wall imaging the sector angle could be narrowed and the myocardial wall could be better aligned to the ultrasound beam during TDI acquisitions. This had two effects, the frame rate could be increased and the angle deviation could be reduced. In rounded hearts, especially basal segments had often an intolerable angle deviation from the ultrasound beam. However, rounded hearts with high end-diastolic volume (EDV) and low ejection fraction (EF) were rare in our studies.

Smoothing provided by QLab, had both a temporal component (weighted averaging of neighboring frames) and spatial smoothing, applied at a ROI of 1cm. The M-mode width was set to 2.5 mm, with the intention to avoid artefacts from blood pool or pericardial tissue due to poorer lateral resolution. The lateral resolution using an iE33 ultrasound scanner (Philips Medical Systems,

Andover, MA) and a S1-4 probe was maximal 56 beams at a full size image. In our studies, frame rates were not increased at a cost of diminishing spatial resolution. Rather the sector angle and image depth were reduced to achieve the highest possible frame rates.

6.11 Artifacts in 2D Strain (Paper II)

The lateral spatial resolution of 2D ultrasound loops is always lower than the perpendicular resolution[4]. Therefore, the method is not completely angle- independent. During one cardiac cycle, speckle patterns change due to out of plane motion, different resolution at different sites or different reflections due to changing fiber orientation towards the probe, causing incorrect tracking. Reverberations and dropouts are similar problems similar to the ones observed in TDI measurements. In both cases, the strain curve is getting flattened giving false positive results for hypokinetic motion. However, increasing noise or higher beat-to-beat variation, like in TDI, does not necessarily occur. Only visual control of correct border tracking and the consequent elimination of regions with artifacts allow reasonable results. In the clinical setting, the dropouts of 2D strains are usually higher when compared to TDI. In the experimental setting using an open chest animal, however, the high-resolution epicardial imaging was nearly free from artifacts; but the correct tracking could only be judged in border regions at the endocardium and epicardium. Visual control was feasible concerning radial total strains, while correct tracking in longitudinal and circumferential direction was not directly accessible to visual control. The only way to control correct tracking in longitudinal or circumferential direction was to follow the tracks of all points in relation to each other. Curves were discarded when the motion of more than 20% of points did not follow a constant track or crossed the track of neighboring points. High spatial resolution was achieved by using an epicardial probe with up to 12 MHz. Frame rates of 100-115 Hz could be attained by reduction of the sector angle and imaging depth without the loss of spatial resolution.

6.12 Extraction of Strain and Strain Rate Data (Paper I-III)

In all three studies, data sets were produced for each segmental measurement with strain and SR values over time. Aortic valve opening and closure were measured on blood flow Doppler in the ascending aorta with simultaneous ECG recordings. Customized software from our study group extracted peak and mean ET-strain, ET-SR values, and calculated post-systolic strain (PSS) and post-systolic index (PSI). Longitudinal ET-strain or SR were defined as either the maximally negative value, the maximally positive or negative value or an averaged value over ET. In a pilot-study, robustness and accuracy of the different strain-data were tested in predicting LE MRI-results in the same hearts. Peak positive or negative ET-strain and mean SR turned out to be the most robust parameters, with the highest accuracy predicting transmural scars. Thus, peak positive or negative strain and mean SR were used in analyses of paper I and III. In paper II layer-strain curves had often both, positive and negative components, especially when flow reductions were induced. Therefore, ET-mean-strain turned out to be the most robust parameter for layer-strain in paper II.

6.13 Post-Prossessing in Paper II

In the second paper, offline dedicated software was used for speckle tracking (Syngo Velocity Vector Imaging, Siemens Medical Systems, Erlangen, Germany). By using the “generic curve” setting the number and position of tracking points could be chosen freely as described in paper II. A data set with all coordinates at all time frames throughout 3 averaged cardiac cycles was used for further analyses. A spatial smoothing algorithm between tracking points was implemented in the software. Coordinates from the images were transformed in a radial-longitudinal or radial-

transversal (circumferential) system. The new coordinate-system was defined by two points in either longitudinal or transversal axes with the radial axis perpendicular.

The following conversion of image (x_{1image}/y_{1image}) coordinates to strain-coordinates ($x_{1strain}/y_{1strain}$) was used:

$$\alpha = \tan (x_b-x_a)/(y_b-y_a)$$

$$\tan \gamma_1 = y_{1image}/ x_{1image}$$

$$\beta_1 = \gamma_1- \alpha$$

$$x_{1\ strain} = x_{1\ image} * (\sin \beta_1/ \sin \gamma_1)$$

$$y_{1\ strain} = x_{1\ strain} *(\tan \beta_1)$$

where ($x_{b/}y_{b)}$ and ($x_{a/}y_a$) are two image-coordinates aligned along the longitudinal or circumferential axis of the strain-coordinate system. α is the angle between the x-axes of both image- and strain-coordinate systems. γ_1 is the angle of the slope between the coordinates ($x_{1/}y_{1\ image)}$ and (0/0) and the x-axis in the image- coordinate system and β_1 is the angle of the same coordinates towards the x-axis (longitudinal or transversal axis) of the strain-coordinate system.

Strain was calculated from either x or y axis strain coordinates, where one axis was either longitudinal or transversal and the perpendicular axis was radial. Thus, analyses of shortening and lengthening were reduced to one dimension. The calculation of strain from the set of coordinates and averaging has been described in paper II. From a dataset with coordinates of each point at each frame, we calculated Lagrangian strain-curves. The end-diastolic distance for calculation of l_0 was defined by distances between points at the time-frame of peak R in the ECG.

7 Results

7.1 Paper I

Left ventricular size determines tissue Doppler derived longitudinal strain and strain rate

The first paper showed a clear dependency of longitudinal strain and SR on heart and body size. The larger individuals displayed lower longitudinal strain values than smaller ones. Additionally, preload increased and afterload decreased radial and longitudinal strain and SR in a closed-chest-model.

7.2 Paper II

High resolution speckle tracking dobutamine stress echocardiography reveals heterogeneous responses in different myocardial layers: implication for viability assessments

In the second paper, the moderate flow reduction at rest (35%) led to strain reduction in all dimensions and layers. Low dose dobutamine stress normalized flow in all layers and activated transmural strains in longitudinal, radial and circumferential direction. Layer strains were significantly increased in mid-myocardial layers in longitudinal and circumferential direction with a moderate correlation to tissue flow. Longitudinal strain revealed the highest sensitivity to dobutamine induced ischemia.

7.3 Paper III

Longitudinal strain in patients with coronary artery disease and preserved ejection fraction. Implications for dobutamine stress echocardiography and tissue Doppler derived strain and strain rate

The patients included were CAD patients undergoing CABG. These patients had predominantly viable myocardium and nearly normal EF. When using longitudinal segmental strain as a measure of myocardial function, 49.9 % of all segments were dysfunctional before CABG. However, only 1.4% of all segments and 3.3 % of all dysfunctional segments displayed transmural scars. Not more than 38% of all dysfunctional segments were improving longitudinal strain after surgery. From all tested parameters, resting ET-strain and DS strain increments were most predictive for functional improvement. The highest probability for improvement was indicated, when DS strain increments were high and resting longitudinal strain positive. Resting strain after CABG improved neither in segments with subendocardial LE positive lesions nor in segments without DSE response. The improvement of segmental function could be predicted with higher accuracies in akinetic than in hypokinetic segments.

8 General discussion

8.1 Strain, SR and the Dependency on Loading

Strain and the influence of loading has been investigated previously[1, 119, 120, 122, 129]. However, since SR correlates mostly with dP/dt and strain with EF, one can assume that SR is the less load-dependent parameter[134]. Additionally, a clinical study has demonstrated the dependency of strain on load changes but not SR[5]. Investigating the load dependency of strain and SR in the closed chest model, it paper I could demonstrate that the curve shape of strain and SR changed substantially. As shown in Figure 3 of paper I, strain at increased afterload had a shallow slope with a late peak at aortic valve closure and increased post-systolic strain. This was paralleled by a SR curve with a late and low ET-peak. The shallow slope with increased post-systolic strain has also been described in hypertensive patients[8].

Instantaneous volume loading in a normal heart leads to increased muscle stretch (Frank-Starling-mechanism) followed by increased contractile force and SV. On cellular basis, preload increases contractile force by lengthening sarcomeres, followed by increasing troponin C calcium sensitivity, which influences the rate of cross-bridge attachment and detachment and thus, the amount of tension developed by the muscle fiber[107]. SV increments are reflected by increased peak ET-strain. A steep slope of the strain-curve also expresses high SR. Of note, during instantaneous volume loading, strain and SR slopes had a delayed onset in contrast to strain curves during dobutamine stress.

Since publication of paper I, a similar study on loading has been performed on patients with recordings of intra-ventricular pressure and echocardiography. In that study, nitrates (GTN) decreased afterload and preload. In accordance with our study, afterload decrease and preload increase led to increased strain and SR values[22].

Loading has an important impact on strain and SR measurements in the clinical setting as loading conditions are changed in most of cardiac diseases: Cardiac dilatation and thinning of myocardial walls lead to increased afterload or wall stress[70]. The rounded shape compensates decreased local wall stress by decreased regional ventricular diameters. Low contractility combined with high wall stress generates low systolic blood pressure (BP_{sys}). At the same time, low mean arterial pressure (MAP) and the rounded shape of the ventricle are compensation mechanisms leading to decreased wall stress[70]. Concentric hypertrophy lowers wall stress by small ventricular cavities and thick myocardial walls[41]. This concentric hypertrophy with small cavities and thick walls allows the left ventricle to generate high pressures[8]. Radial strain increases, whereas longitudinal strain decreases in hypertensive patients[121] and in ageing hearts, where the arterial impedance increases due to higher arterial stiffness[74]. Thus, strain and SR in the clinical setting have to be interpreted with care, considering a variety of factors influencing individual measurements.

8.2 Strain and SR and Heart Size?

The dependency of longitudinal strain and SR on heart and/or body size has been demonstrated in Paper I. Heart rate can influence strain and SR indirectly by a reduced filling time at shortened diastoles. This factor in this study could be controlled by pacing all pigs at the same heart rate. The results of Paper I were in accordance with population studies, showing lower strain and SR values with increasing BMI[55, 74]. A recent study compared obese with normal individuals observing significantly lower strain and SR values in the group with a BMI over 30kg/m^2, while EF stayed unchanged[97]. The explanation to these phenomena remains a challenging subject. Several observations indicate that contractility is not affected by increasing BMI. As mentioned before,

Dogs of different sizes had unchanged stress-strain relationship as indicator for unchanged contractility[94].

Additional data from our laboratory from 30 open chest pigs of varying sizes included body weight, resting cardiac output (CO), heart rate and continuous intraventricular pressures and MAP. By calculating vascular resistance from the ratio of MAP-venous pressure and CO, vascular resistance corrected for body weight was clearly lower and CO and SV corrected for body weight were higher in smaller individuals. Thus, peripheral vascular resistance related to body weight, might explain higher strain and SR in smaller individuals. However, this does not answer the question about the cause of varying vascular resistance. One explanation might be lower aortic dispensability in larger individuals. Some studies on healthy or obese children indicate increasing arterial stiffness with obesity, but no correlation with age alone[58, 79, 139].

In the next paragraph, another hypothetical reason for reduced arterial resistance in smaller individuals is being discussed: The body surface represents the skin, the biggest human organ with a vast capillary bed. This might explain why vascular resistance and CO correlate with body-surface-area (BSA) in normotensive children and adults[33, 114]. However, it is known and we could show in our study, that cardiac size in mammals increases in 1:1 correlation to (the ideal) body weight[108] and not to CO. Main hemodynamic changes between smaller and bigger individuals might therefore be the ratio between BSA and body weight. When weight increases in the third dimension, BSA increases in the second dimension. Thus, mice have a much higher BSA/weight ratio than elephants. In other words, mice have a higher CO/heart size, probably due to a lower peripheral resistance/heart size. This changed ratio is reflected by decreasing heart rate in growing children or a heart rate around 600/min in mice contra 35-40 /min in elephants[108]. A lower vascular resistance-body weight ratio at a constant heart rate might be the main cause for higher longitudinal strains in our experiments.

8.3 Strain and Flow during Dobutamine Stress

In paper II a constant critical stenosis was applied with 35% flow reduction in the left anterior descending (LAD)-artery. This setting was crucial to obtain decreased strain at rest and preserve flow reserve under low dose dobutamine. These conditions allowed dobutamine to increase flow in the stenotic vessel, probably due to further decrease in peripheral vascular resistance. Thus, constant maximal ischemic vasodilatation was not reached at a 35% resting-flow reduction. Interestingly, dobutamine increased flow beyond resting values in the lateral non-ischemic wall, whereas in the same region, neither strain nor global hemodynamic parameters increased beyond initial values. However, LAD constriction was followed by reduction in global hemodynamic parameters like SV, CO, BP_{sys} and MAP. Dobutamine application normalized the hemodynamic parameters and seemed to have a higher impact on ET-strain in the ischemic than in the neighboring area. This might reflect the dependency of regional strain on global cardiac function and changes in global wall stress and not on regional flow alone.

Figure 3 in Paper II demonstrates strain changes in the various layers of the myocardium during LAD flow reductions followed by low dose dobutamine. Interestingly, during dobutamine infusion the midmyocardial circumferential layer showed higher (negative) strains than the subendocardial layer. One would expect that subendocardial circumferential strain should deform equally to midmyocardial strain due to tethering of neighboring layers. However, circumferential strain seemed to reflect the regionally depressed contractile state of the subendocardium despite tethering to an active contracting layer.

Figure 3 demonstrates strain in different myocardial layers during flow reduction and dobutamine challenge. Subendocardial strains in longitudinal and circumferential direction were not different from strains at flow reduction, while the (non-significant) increment of subendocardial radial strain might indicate contraction. However, it is possible that the “activation” of subendocardial radial strain mainly reflects the effect of cross fiber activation of mid-myocardial

layers in circumferential direction[17, 102]. This observation leads to the conclusion that dobutamine does not activate subendocardial hypoperfused in neither direction, in contrast to mid-subendocardial and mid-subepicardial layers in longitudinal and circumferential direction. This finding implicates a potential of high resolution DSE to identify viability in mid-myocardial layers.

Results from Paper II were dependent on the use of dobutamine-doses of 2.5 $\mu gkg^{-1}min^{-1}$. If the dose response was comparable to humans the results would indicate that viability testing with a dobutamine dose of 2.5-5 $\mu gkg^{-1}min^{-1}$ might result in higher sensitivities detecting viable, ischemic tissue.

8.4 Positioning of the Region of Interest

In some clinical studies, radial strain, measured mid-myocardially yielded higher variances and intra- and inter-observer variabilities than longitudinal strain[13, 26]. In our experimental setting, this might be partially due to a higher spatial resolution in longitudinal strain. Additionally, it could be suspected that the strain-gradients inside the myocardial wall influence the measurements according to the position of the ROI. As shown in our data, the radial direction exhibits the highest strain gradients. These gradients increase with higher wall curvatures, for instance in the posterolateral wall where radial strains are measured in TDI-studies. Analysis of TDI data in 2 mm long segments sometimes resulted in partially negative radial strain. This could happen when the ROI was displaced during one cardiac cycle from one layer with high strains towards a layer with low strains. Automated tracking of the ROI might help avoiding this error, but it does not prevent achieving differing results when investigators vary initial ROI positions inside the myocardial wall.

2D strain methods based on border detection in the subendocardium and subepicardium might underestimate strain increments or decrements in all directions by not registering midmyocardial strains where dobutamine-response of viable myocardium is highest. According to the results from

paper II, longitudinal TDI strain, positioned mid-myocardially might have the highest potential to differentiating ischemic substrates.

8.5 Recovery of Function and Viability

Kim *et al.* used LE-MRI in a patient population with low EF and a high number of ischemic scars. In this study global functional improvement was present in nearly all patients with a majority of viable segments[71]. One study on patients with known wall motion abnormalities and mean EF of 39% identified improvement of segmental radial function by cine-MRI. LE-negative segments improved in 80% after 6 months and 95% after 2 years. Other MRI-studies combined with strain-measurements and WMS improvement reported similar high functional recovery rates of LE-negative segments[14, 109]. Other publications on segmental strain and functional recovery investigated a ratio of 20% LE-negative to 80% LE-positive dysfunctional segments, whereas the total number of dysfunctional segments in paper III was around 50%[14, 71, 109]. In contrast to these studies, in the patient population of paper III, EF was nearly normal and the number of LE-positive segments was low. However, measuring longitudinal strain revealed still 50% dysfunctional segments wherefrom 86% were LE-negative. From this high number of dysfunctional but viable segments, defined by LE-MRI only 38% improved function, even though the number of ischemic scars in dysfunctional segments was low (3.3% transmural scars and 12.8% non-transmural scars). However, there are several possible explanations of the differing results:

1. The time course of functional recovery might be an important factor. Long-term follow ups demonstrated that delayed recovery may occur up to 12-24 months[2, 20, 29]. However, the same studies showed already much higher recovery rates for LE-negative dysfunctional segments at a 6-9 months period. In paper III functional recovery was investigated 9 months (8-10) after CABG.

2. Hibernation studies have so far either assessed global functional recovery by EF measurements (by echocardiography or MRI) or regional myocardial functional assessments by

WMS or wall thickening in cine-MRI studies[9-12, 14, 52, 60, 95, 106, 109, 131]. All these methods are mainly based on the functional recovery of radial function. To my knowledge, longitudinal regional function has not been used to this date to define functional recovery after revascularization. As shown in Paper II, longitudinal strain seems to be more sensitive to minor ischemic lesions. Additionally, longitudinal strain might recover to a lesser extent than radial strain due to higher amount of damage of the subendocardial longitudinal fibers in CAD. Therefore longitudinal strain would be expected to be more sensitive to long-term myocardial dysfunction than radial strain[26]. However, when assessing WMS and strain in the same patients, the number of segments defined as dysfunctional by either method was not substantially different. This might be due to the subjective component in assessing WMS and the expectation of the observer to detect an equal amount of dysfunctional segments by WMS as by strain-measurements. In some patients, apical and medial wall thickening was considered as dysfunctional, when longitudinal stretching was observed at the same time, resulting in pathological rotation of apical segments in apical views.

3. In the study of Becker *et al.*[14] 45% of segments displayed scar tissue, and not more than 5% of segments were dysfunctional and LE-negative. One could assume that these few unscarred dysfunctional segments were mainly positioned in ischemic border-zones, whereas scar-tissue was mainly positioned in the centers of ischemic lesions. Tissue from border-zones might comprise low ischemic damage and thus high potential to increase function after revascularization. In our study-population, the distribution of viable, dysfunctional myocardium was probably ranging from the center of ischemic areas to border zones. As described earlier, biopsies of dysfunctional viable myocardium have shown all degrees of myocardial damage. It seems possible, that normal function cannot be restored when high grade diffuse apoptosis and scattered myocardial damage is present despite the absence of visible scar tissue. Thus in paper III, the high variance of diffuse structural disorders and distribution across all zones of ischemic areas might explain the low number of recovery in viable, dysfunctional segments.

4. In addition to structural disorders, there might be other factors explaining functional non-recovery of viable myocardium. Wall stress changing due to remodeling, re-remodeling or the effect of medical therapy might have their own effects on deteriorating or improving myocardial deformation parameters unrelated to complete or incomplete revascularization[19]. Most studies addressing viability-assessment have included patients with very low EF[9-12, 14, 52, 60, 95, 106, 109, 131]. In those patient-populations, not all of dysfunctional segments have to increase function to initiate the re-remodeling process[27, 104]. When EDV decreases, wall stress decreases, EF raises and regional myocardial deformation can improve even in segments where contractile function stays unchanged. However, only when loading conditions stay unchanged after revascularization, segmental deformation parameters and WMS will express true segmental functional recovery. Thus, when re-remodeling occurs, regional functional improvement expresses either decreased wall stress, increased segmental contractility or both.

In contrast to most of viability studies, Paper III investigated a patient population with nearly normal EF, a low number of transmural and subendocardial scars and no significant changes of EDV, EF, E/E`, E deceleration time or E velocity after CABG. These values indicated no re-remodeling and no differences in filling pressures or loading conditions of the left ventricle after surgery. Therefore, in this study where postoperative loading conditions stayed unchanged, strain improvements reflect most likely improvement of regional contractility.

8.6 Prediction of Functional Recovery

Prediction of functional recovery in Paper III was possible with good to fair results, even though the detection of LE-negative segments without the potential of functional recovery is much more challenging than the identification of transmural scar tissue. Of all tested parameters, resting strain and DSE-strain increment correlated best with the amount of functional recovery. Either high or low DSE-values gave conclusive results. However, the predictive value for functional recovery

in segments with moderate DSE increments was low. Resting strain might be favored as a factor, by using longitudinal resting strain as indicator for functional improvement. Our data indicated that segments with positive strain had high probability to improve and normalize resting function. Tissue elasticity was preserved when resting strains had positive values and DSE-strain-increments were high. Akinesia included “positive strain”, resulting in better predictive accuracies for functional improvement than hypokinetic segments, where the factor “positive strain” was excluded by definition.

9 Conclusions

1. Heart or body size influence longitudinal strain and SR. Loading conditions always have to be taken into account when interpreting individual strain and SR values in the clinical setting.

2. Dobutamine infusions during a constant coronary stenosis influence heterogeneously layer strains in different dimensions. Using speckle tracking or TDI strain methods have to take into account that regions of interest placed at different layers of the myocardium might yield varying results. Mid-subendocardial layers activated by low dose dobutamine might have the potential to be used as regional viability markers.

3. In CAD-patients with predominantly viable segments and nearly normal EF, half of all segments display reduced preoperative longitudinal function. More than half of all dysfunctional segments do not improve resting longitudinal function after CABG. The combination of resting strain and DSE-strain-increments allows identifying segments improving after CABG with fair results. Segments with positive longitudinal strains have preserved tissue elasticity and high chances to restore function after CABG.

10 Future Perspectives

Several aspects have to be addressed concerning the establishment of SRI in the routine clinical use:

Firstly, the definitions of normal values and cut-off values are to be agreed upon. Several population studies have defined normal values in children and adults[16, 31, 79]. However, unpublished data indicate profound intertechnique variabilities in dependency on the system and software used. Only defining normal values for each system and software and/or implying standard procedures for data processing in SRI can solve this problem. However, even if the technical differences could be overcome, normal values will still have to be defined for different ages, races, obese and slim, athletes, children, pregnant women, and fetuses. Even if contractility stays normal, geometry, vascular resistance and loading vary substantially between these groups, and all these factors are influencing normal strains. Additionally, changes in hypertensive, obese, diabetic or atherosclerotic individuals and valvular- or congenital heart disease, will have to be defined as physiological conditions or pathological values. For the use as a bedside test the degree of strain increments or decrements or differences between segments that indicate a pathological state have to be accurately evaluated.

Secondly, strain is only a deformation parameter, and not a strict contractility-marker. When loading varies substantially, strain and SR always express the sum of varying wall stress, preload and contractile state. Cardiogenic shock and the use of positive inotrope substances is a good example where neither blood pressure nor strain alone can monitor the optimal treatment. Stress strain algorithms[88, 94] by using continuous blood pressures and strains at ET combined with calculation of arterial elastance[69, 98] might give a closer approach to reflecting myocardial contractility.

Finally, SRI has the potential to be established as a more sensitive marker for myocardial dysfunction than the widely use of EF. It has already been shown, that strain and SR reduction

precedes EF reduction or visible myocardial fibrosis[24, 46, 47, 133, 136]. For example, the time point for operative treatment of asymptomatic valve diseases might be supported by SRI assessment[25, 37, 75, 82, 83, 115]. Cardiomyopathies[40, 140, 141] could be detected earlier and the time course of cardiomyopathies and the use of cardiotoxic substances[46, 47, 66, 67, 99] could be monitored with a higher precision.

To answer all these questions might be the work of the next decades. However, many examples have shown already today, that, interpreted with care, SRI can be used as a valuable supportive tool in clinical decision-making.

11 Reference List

(1) Abraham TP, Laskowski C, Zhan WZ et al. Myocardial contractility by strain echocardiography: comparison with physiological measurements in an in vitro model. *Am J Physiol Heart Circ Physiol* 2003 December;285(6):H2599-H2604.

(2) Alfieri O, La Canna G, Giubbini R, Pardini A, Zogno M, Fucci C. Recovery of myocardial function. The ultimate target of coronary revascularization. *Eur J Cardiothorac Surg* 1993;7(6):325-30.

(3) Amundsen BH, Crosby J, Steen PA, Torp H, Slordahl SA, Stoylen A. Regional myocardial long-axis strain and strain rate measured by different tissue Doppler and speckle tracking echocardiography methods: a comparison with tagged magnetic resonance imaging 2. *Eur J Echocardiogr* 2008 July 23.

(4) Amundsen BH, Helle-Valle T, Edvardsen T et al. Noninvasive myocardial strain measurement by speckle tracking echocardiography: validation against sonomicrometry and tagged magnetic resonance imaging. *J Am Coll Cardiol* 2006 February 21;47(4):789-93.

(5) Andersen NH, Terkelsen CJ, Sloth E, Poulsen SH. Influence of preload alterations on parameters of systolic left ventricular long-axis function: a Doppler tissue study. *J Am Soc Echocardiogr* 2004 September;17(9):941-7.

(6) Ashikaga H, Coppola BA, Hopenfeld B, Leifer ES, McVeigh ER, Omens JH. Transmural dispersion of myofiber mechanics: implications for electrical heterogeneity in vivo. *J Am Coll Cardiol* 2007 February 27;49(8):909-16.

(7) Bache RJ, McHale PA, Greenfield JC, Jr. Transmural myocardial perfusion during restricted coronary inflow in the awake dog. *Am J Physiol* 1977 June;232(6):H645-H651.

(8) Baltabaeva A, Marciniak M, Bijnens B et al. Regional left ventricular deformation and geometry analysis provides insights in myocardial remodelling in mild to moderate hypertension. *Eur J Echocardiogr* 2008 July;9(4):501-8.

(9) Bax JJ. Assessment of myocardial viability in ischemic cardiomyopathy. *Heart Lung Circ* 2005;14 Suppl 2:S8-13.

(10) Bax JJ, de Roos A, Der Wall EE. Assessment of myocardial viability by MRI. *J Magn Reson Imaging* 1999 September;10(3):418-22.

(11) Bax JJ, Poldermans D, Elhendy A, Boersma E, Rahimtoola SH. Sensitivity, specificity, and predictive accuracies of various noninvasive techniques for detecting hibernating myocardium. *Curr Probl Cardiol* 2001 February;26(2):147-86.

(12) Bax JJ, van der Wall EE, Harbinson M. Radionuclide techniques for the assessment of myocardial viability and hibernation. *Heart* 2004 August;90 Suppl 5:v26-v33.

(13) Becker M, Bilke E, Kuhl H et al. Analysis of myocardial deformation based on pixel tracking in two dimensional echocardiographic images enables quantitative assessment of regional left ventricular function. *Heart* 2006 August;92(8):1102-8.

(14) Becker M, Lenzen A, Ocklenburg C et al. Myocardial deformation imaging based on ultrasonic pixel tracking to identify reversible myocardial dysfunction. *J Am Coll Cardiol* 2008 April 15;51(15):1473-81.

(15) Bijnens B, Claus P, Weidemann F, Strotmann J, Sutherland GR. Investigating cardiac function using motion and deformation analysis in the setting of coronary artery disease. *Circulation* 2007 November 20;116(21):2453-64.

(16) Boettler P, Hartmann M, Watzl K et al. Heart rate effects on strain and strain rate in healthy children. *J Am Soc Echocardiogr* 2005 November;18(11):1121-30.

(17) Bogaert J, Rademakers FE. Regional nonuniformity of normal adult human left ventricle. *Am J Physiol Heart Circ Physiol* 2001 February;280(2):H610-H620.

(18) Bohs LN, Trahey GE. A novel method for angle independent ultrasonic imaging of blood flow and tissue motion. *IEEE Trans Biomed Eng* 1991 March;38(3):280-6.

(19) Bolognese L, Neskovic AN, Parodi G et al. Left ventricular remodeling after primary coronary angioplasty: patterns of left ventricular dilation and long-term prognostic implications. *Circulation* 2002 October 29;106(18):2351-7.

(20) Bondarenko O, Beek AM, Twisk JW, Visser CA, van Rossum AC. Time course of functional recovery after revascularization of hibernating myocardium: a contrast-enhanced cardiovascular magnetic resonance study. *Eur Heart J* 2008 August;29(16):2000-5.

(21) Brown MA, Norris RM, Takayama M, White HD. Post-systolic shortening: a marker of potential for early recovery of acutely ischaemic myocardium in the dog. *Cardiovasc Res* 1987 October;21(10):703-16.

(22) Burns AT, La Gerche A, D'hooge J, Macisaac AI, Prior DL. Left ventricular strain and strain rate: characterization of the effect of load in human subjects. *Eur J Echocardiogr* 2009 December 20.

(23) Butterfield TA, Herzog W. Quantification of muscle fiber strain during in vivo repetitive stretch-shortening cycles. *J Appl Physiol* 2005 August;99(2):593-602.

(24) Buyse G, Mertens L, Di Salvo G et al. Idebenone treatment in Friedreich's ataxia: neurological, cardiac, and biochemical monitoring. *Neurology* 2003 May 27;60(10):1679-81.

(25) Carlhall CJ, Nguyen TC, Itoh A et al. Alterations in transmural myocardial strain: an early marker of left ventricular dysfunction in mitral regurgitation? *Circulation* 2008 September 30;118(14 Suppl):S256-S262.

(26) Chan J, Hanekom L, Wong C, Leano R, Cho GY, Marwick TH. Differentiation of subendocardial and transmural infarction using two-dimensional strain rate imaging to assess short-axis and long-axis myocardial function. *J Am Coll Cardiol* 2006 November 21;48(10):2026-33.

(27) Chan J, Khafagi F, Young AA, Cowan BR, Thompson C, Marwick TH. Impact of coronary revascularization and transmural extent of scar on regional left ventricular remodelling. *Eur Heart J* 2008 July;29(13):1608-17.

(28) Chen J, Liu W, Zhang H et al. Regional ventricular wall thickening reflects changes in cardiac fiber and sheet structure during contraction: quantification with diffusion tensor MRI. *Am J Physiol Heart Circ Physiol* 2005 November;289(5):H1898-H1907.

(29) Cornel JH, Bax JJ, Elhendy A et al. Biphasic response to dobutamine predicts improvement of global left ventricular function after surgical revascularization in patients with stable coronary artery disease: implications of time course of recovery on diagnostic accuracy. *J Am Coll Cardiol* 1998 April;31(5):1002-10.

(30) Costa KD, Takayama Y, McCulloch AD, Covell JW. Laminar fiber architecture and three-dimensional systolic mechanics in canine ventricular myocardium. *Am J Physiol* 1999 February;276(2 Pt 2):H595-H607.

(31) Dalen H, Thorstensen A, Aase SA et al. Segmental and global longitudinal strain and strain rate based on echocardiography of 1266 healthy individuals: the HUNT study in Norway. *Eur J Echocardiogr* 2009 November 28.

(32) Dalmas S, Wanigasekera VA, Marsch SC, Ryder WA, Wong LS, Foex P. The influence of preload on post-systolic shortening in ischaemic myocardium. *Eur J Anaesthesiol* 1995 March;12(2):127-33.

(33) de Simone G, Devereux RB, Daniels SR et al. Stroke volume and cardiac output in normotensive children and adults. Assessment of relations with body size and impact of overweight. *Circulation* 1997 April 1;95(7):1837-43.

(34) Delhaas T, Arts T, Bovendeerd PH, Prinzen FW, Reneman RS. Subepicardial fiber strain and stress as related to left ventricular pressure and volume. *Am J Physiol* 1993 May;264(5 Pt 2):H1548-H1559.

(35) Derumeaux G, Ovize M, Loufoua J et al. Doppler tissue imaging quantitates regional wall motion during myocardial ischemia and reperfusion. *Circulation* 1998 May 19;97(19):1970-7.

(36) Derumeaux G, Ovize M, Loufoua J, Pontier G, Andre-Fouet X, Cribier A. Assessment of nonuniformity of transmural myocardial velocities by color-coded tissue Doppler imaging: characterization of normal, ischemic, and stunned myocardium. *Circulation* 2000 March 28;101(12):1390-5.

(37) Di Salvo G, Pacileo G, Verrengia M et al. Early myocardial abnormalities in asymptomatic patients with severe isolated congenital aortic regurgitation: an ultrasound tissue characterization and strain rate study. *J Am Soc Echocardiogr* 2005 February;18(2):122-7.

(38) Douglas AS, Rodriguez EK, O'Dell W, Hunter WC. Unique strain history during ejection in canine left ventricle. *Am J Physiol* 1991 May;260(5 Pt 2):H1596-H1611.

(39) Edvardsen T, Gerber BL, Garot J, Bluemke DA, Lima JA, Smiseth OA. Quantitative assessment of intrinsic regional myocardial deformation by Doppler strain rate echocardiography in humans: validation against three-dimensional tagged magnetic resonance imaging. *Circulation* 2002 July 2;106(1):50-6.

(40) Edwards NC, Hirth A, Ferro CJ, Townend JN, Steeds RP. Subclinical abnormalities of left ventricular myocardial deformation in early-stage chronic kidney disease: the precursor of uremic cardiomyopathy? *J Am Soc Echocardiogr* 2008 December;21(12):1293-8.

(41) Fischl SJ, Gorlin R, Herman MV. Cardiac shape and function in aortic valve disease: physiologic and clinical implications. *Am J Cardiol* 1977 February;39(2):170-6.

(42) Fleming AD, McDicken WN, Sutherland GR, Hoskins PR. Assessment of colour Doppler tissue imaging using test-phantoms. *Ultrasound Med Biol* 1994;20(9):937-51.

(43) Gallagher KP, Kumada T, Koziol JA, McKown MD, Kemper WS, Ross J, Jr. Significance of regional wall thickening abnormalities relative to transmural myocardial perfusion in anesthetized dogs. *Circulation* 1980 December;62(6):1266-74.

(44) Gallagher KP, Matsuzaki M, Koziol JA, Kemper WS, Ross J, Jr. Regional myocardial perfusion and wall thickening during ischemia in conscious dogs. *Am J Physiol* 1984 November;247(5 Pt 2):H727-H738.

(45) Gallagher KP, Stirling MC, Choy M et al. Dissociation between epicardial and transmural function during acute myocardial ischemia. *Circulation* 1985 June;71(6):1279-91.

(46) Ganame J, Claus P, Eyskens B et al. Acute cardiac functional and morphological changes after Anthracycline infusions in children. *Am J Cardiol* 2007 April 1;99(7):974-7.

(47) Ganame J, Claus P, Uyttebroeck A et al. Myocardial dysfunction late after low-dose anthracycline treatment in asymptomatic pediatric patients. *J Am Soc Echocardiogr* 2007 December;20(12):1351-8.

(48) Gorcsan J, III, Gulati VK, Mandarino WA, Katz WE. Color-coded measures of myocardial velocity throughout the cardiac cycle by tissue Doppler imaging to quantify regional left ventricular function. *Am Heart J* 1996 June;131(6):1203-13.

(49) Greenbaum RA, Ho SY, Gibson DG, Becker AE, Anderson RH. Left ventricular fibre architecture in man. *Br Heart J* 1981 March;45(3):248-63.

(50) Guccione JM, O'Dell WG, McCulloch AD, Hunter WC. Anterior and posterior left ventricular sarcomere lengths behave similarly during ejection. *Am J Physiol* 1997 January;272(1 Pt 2):H469-H477.

(51) Guth BD, Schulz R, Heusch G. Time course and mechanisms of contractile dysfunction during acute myocardial ischemia. *Circulation* 1993 May;87(5 Suppl):IV35-IV42.

(52) Hanekom L, Jenkins C, Jeffries L et al. Incremental value of strain rate analysis as an adjunct to wall-motion scoring for assessment of myocardial viability by dobutamine echocardiography: a follow-up study after revascularization. *Circulation* 2005 December 20;112(25):3892-900.

(53) Hashimoto I, Li X, Hejmadi BA, Jones M, Zetts AD, Sahn DJ. Myocardial strain rate is a superior method for evaluation of left ventricular subendocardial function compared with tissue Doppler imaging. *J Am Coll Cardiol* 2003 November 5;42(9):1574-83.

(54) Heimdal A, Stoylen A, Torp H, Skjaerpe T. Real-time strain rate imaging of the left ventricle by ultrasound. *J Am Soc Echocardiogr* 1998 November;11(11):1013-9.

(55) Herbots L. Quantification of regional myocardial deformation; normal characteristics and clinical use in ischaemic heart disease. 1-133. 2006. Acta biomedica loveniensia 370, Leuven University Press.

(56) Heusch G, Schulz R. Hibernating myocardium: new answers, still more questions! *Circ Res* 2002 November 15;91(10):863-5.

(57) Heyndrickx GR, Millard RW, McRitchie RJ, Maroko PR, Vatner SF. Regional myocardial functional and electrophysiological alterations after brief coronary artery occlusion in conscious dogs. *J Clin Invest* 1975 October;56(4):978-85.

(58) Hlaing WM, Prineas RJ. Arterial stiffness variations by gender in African-American and Caucasian children. *J Natl Med Assoc* 2006 February;98(2):181-9.

(59) Hoffmann R, Lethen H, Marwick T et al. Analysis of interinstitutional observer agreement in interpretation of dobutamine stress echocardiograms. *J Am Coll Cardiol* 1996 February;27(2):330-6.

(60) Hoffmann R, Stempel K, Kuhl H et al. Integrated analysis of cardiac tissue structure and function for improved identification of reversible myocardial dysfunction. *Coron Artery Dis* 2009 January;20(1):21-6.

(61) Ihara T, Komamura K, Shen YT et al. Left ventricular systolic dysfunction precedes diastolic dysfunction during myocardial ischemia in conscious dogs. *Am J Physiol* 1994 July;267(1 Pt 2):H333-H343.

(62) Ingul B.C., Rozis E, Slordahl SA, Marwick TH. Incremental value of strain rate imaging to wall motion analysis for prediction of outcome in patients undergoing dobutamine stress echocardiography. *Circulation* 2007 March 13;115(10):1252-9.

(63) Isaaz K, Thompson A, Ethevenot G, Cloez JL, Brembilla B, Pernot C. Doppler echocardiographic measurement of low velocity motion of the left ventricular posterior wall. *Am J Cardiol* 1989 July 1;64(1):66-75.

(64) Jamal F, Kukulski T, Strotmann J et al. Quantification of the spectrum of changes in regional myocardial function during acute ischemia in closed chest pigs: an ultrasonic strain rate and strain study. *J Am Soc Echocardiogr* 2001 September;14(9):874-84.

(65) Jamal F, Strotmann J, Weidemann F et al. Noninvasive quantification of the contractile reserve of stunned myocardium by ultrasonic strain rate and strain. *Circulation* 2001 August 28;104(9):1059-65.

(66) Jurcut R, Wildiers H, Ganame J et al. Strain rate imaging detects early cardiac effects of pegylated liposomal Doxorubicin as adjuvant therapy in elderly patients with breast cancer. *J Am Soc Echocardiogr* 2008 December;21(12):1283-9.

(67) Jurcut R, Wildiers H, Ganame J, D'hooge J, Paridaens R, Voigt JU. Detection and monitoring of cardiotoxicity-what does modern cardiology offer? *Support Care Cancer* 2008 May;16(5):437-45.

(68) Kaluzynski K, Chen X, Emelianov SY, Skovoroda AR, O'Donnell M. Strain rate imaging using two-dimensional speckle tracking. *IEEE Trans Ultrason Ferroelectr Freq Control* 2001 July;48(4):1111-23.

(69) Kass DA. Age-related changes in venticular-arterial coupling: pathophysiologic implications. *Heart Fail Rev* 2002 January;7(1):51-62.

(70) Kass DA, Traill TA, Keating M, Altieri PI, Maughan WL. Abnormalities of dynamic ventricular shape change in patients with aortic and mitral valvular regurgitation: assessment by Fourier shape analysis and global geometric indexes. *Circ Res* 1988 January;62(1):127-38.

(71) Kim RJ, Wu E, Rafael A et al. The use of contrast-enhanced magnetic resonance imaging to identify reversible myocardial dysfunction. *N Engl J Med* 2000 November 16;343(20):1445-53.

(72) Kjorstad KE, Korvald C, Myrmel T. Pressure-volume-based single-beat estimations cannot predict left ventricular contractility in vivo. *Am J Physiol Heart Circ Physiol* 2002 May;282(5):H1739-H1750.

(73) Kowallik P, Schulz R, Guth BD et al. Measurement of regional myocardial blood flow with multiple colored microspheres. *Circulation* 1991 March;83(3):974-82.

(74) Kuznetsova T, Herbots L, Richart T et al. Left ventricular strain and strain rate in a general population. *Eur Heart J* 2008 August;29(16):2014-23.

(75) Lancellotti P, Cosyns B, Zacharakis D et al. Importance of left ventricular longitudinal function and functional reserve in patients with degenerative mitral regurgitation: assessment by two-dimensional speckle tracking. *J Am Soc Echocardiogr* 2008 December;21(12):1331-6.

(76) Langer F, Rodriguez F, Cheng A et al. Alterations in lateral left ventricular wall transmural strains during acute circumflex and anterior descending coronary occlusion. *Ann Thorac Surg* 2007 July;84(1):51-60.

(77) Lee DC, Johnson NP. Quantification of absolute myocardial blood flow by magnetic resonance perfusion imaging. *JACC Cardiovasc Imaging* 2009 June;2(6):761-70.

(78) Leone BJ, Norris RM, Safwat A, Foex P, Ryder WA. Effects of progressive myocardial ischaemia on systolic function, diastolic dysfunction, and load dependent relaxation. *Cardiovasc Res* 1992 April;26(4):422-9.

(79) Levent E, Goksen D, Ozyurek AR et al. Stiffness of the abdominal aorta in obese children. *J Pediatr Endocrinol Metab* 2002 April;15(4):405-9.

(80) Lunkenheimer PP, Redmann K, Kling N et al. Three-dimensional architecture of the left ventricular myocardium. *Anat Rec A Discov Mol Cell Evol Biol* 2006 June;288(6):565-78.

(81) Mailloux GE, Bleau A, Bertrand M, Petitclerc R. Computer analysis of heart motion from two-dimensional echocardiograms. *IEEE Trans Biomed Eng* 1987 May;34(5):356-64.

(82) Marciniak A, Claus P, Sutherland GR et al. Changes in systolic left ventricular function in isolated mitral regurgitation. A strain rate imaging study. *Eur Heart J* 2007 November;28(21):2627-36.

(83) Marciniak A, Sutherland GR, Marciniak M, Claus P, Bijnens B, Jahangiri M. Myocardial deformation abnormalities in patients with aortic regurgitation: a strain rate imaging study. *Eur J Echocardiogr* 2009 January;10(1):112-9.

(84) Marwick TH. Current status of stress echocardiography for diagnosis and prognostic assessment of coronary artery disease
1. *Coron Artery Dis* 1998;9(7):411-26.

(85) Matre K, Fannelop T, Dahle GO, Heimdal A, Grong K. Radial strain gradient across the normal myocardial wall in open-chest pigs measured with doppler strain rate imaging. *J Am Soc Echocardiogr* 2005 October;18(10):1066-73.

(86) Matre K, Moen CA, Fannelop T, Dahle GO, Grong K. Multilayer radial systolic strain can identify subendocardial ischemia: An experimental tissue Doppler imaging study of the porcine left ventricular wall. *Eur J Echocardiogr* 2007 December;8(6):420-30.

(87) Mazhari R, Omens JH, Waldman LK, McCulloch AD. Regional myocardial perfusion and mechanics: a model-based method of analysis. *Ann Biomed Eng* 1998 September;26(5):743-55.

(88) Mc Laughlin M, Claus P, Mehwald P et al. A model based approach to estimate contractile force development using myocardial velocity imaging: a validation study during alterations in contractility and heart rate. IEEE International Ultrasonics, Ferroelectrics and Frequency Control Joint 50th Aniversary Conferences , 478-481. 2004.

(89) Meier GD, Ziskin MC, Bove AA. Helical fibers in myocardium of dogs change their pitch as they contract. *Am J Physiol* 1982 July;243(1):H1-12.

(90) Mirsky I, Parmley WW. Assessment of passive elastic stiffness for isolated heart muscle and the intact heart. *Circ Res* 1973 August;33(2):233-43.

(91) Miyatake K, Yamagishi M, Tanaka N et al. New method for evaluating left ventricular wall motion by color-coded tissue Doppler imaging: in vitro and in vivo studies. *J Am Coll Cardiol* 1995 March 1;25(3):717-24.

(92) Moon BR, Conley KE, Lindstedt SL, Urquhart MR. Minimal shortening in a high-frequency muscle. *J Exp Biol* 2003 April;206(Pt 8):1291-7.

(93) Moore CC, Lugo-Olivieri CH, McVeigh ER, Zerhouni EA. Three-dimensional systolic strain patterns in the normal human left ventricle: characterization with tagged MR imaging. *Radiology* 2000 February;214(2):453-66.

(94) Nakano K, Sugawara M, Ishihara K et al. Myocardial stiffness derived from end-systolic wall stress and logarithm of reciprocal of wall thickness. Contractility index independent of ventricular size. *Circulation* 1990 October;82(4):1352-61.

(95) Nelson C, Marwick TH. Clinical decision-making and myocardial viability: current perspectives. *Intern Med J* 2005 February;35(2):118-25.

(96) Opie LH. Regulation of myocardial contractility. *J Cardiovasc Pharmacol* 1995;26 Suppl 1:S1-S9.

(97) Orhan AL, Uslu N, Dayi SU et al. Effects of Isolated Obesity on Left and Right Ventricular Function: A Tissue Doppler and Strain Rate Imaging Study. *Echocardiography* 2010 January 13.

(98) Osranek M, Eisenach JH, Khandheria BK, Chandrasekaran K, Seward JB, Belohlavek M. Arterioventricular coupling and ventricular efficiency after antihypertensive therapy: a noninvasive prospective study. *Hypertension* 2008 February;51(2):275-81.

(99) Piegari E, Di Salvo G, Castaldi B et al. Myocardial strain analysis in a doxorubicin-induced cardiomyopathy model. *Ultrasound Med Biol* 2008 March;34(3):370-8.

(100) Pislaru C, Bruce CJ, Seward JB, Greenleaf JF. Distinctive changes in end-diastolic wall thickness and postsystolic thickening in viable and infarcted myocardium. *J Am Soc Echocardiogr* 2004 August;17(8):855-62.

(101) Prinzen FW, Arts T, van der Vusse GJ, Reneman RS. Fiber shortening in the inner layers of the left ventricular wall as assessed from epicardial deformation during normoxia and ischemia. *J Biomech* 1984;17(10):801-11.

(102) Rademakers FE, Rogers WJ, Guier WH et al. Relation of regional cross-fiber shortening to wall thickening in the intact heart. Three-dimensional strain analysis by NMR tagging. *Circulation* 1994 March;89(3):1174-82.

(103) Rahimtoola SH. The hibernating myocardium. *Am Heart J* 1989 January;117(1):211-21.

(104) Rizzello V, Poldermans D, Biagini E et al. Prognosis of patients with ischaemic cardiomyopathy after coronary revascularisation: relation to viability and improvement in left ventricular ejection fraction. *Heart* 2009 August;95(15):1273-7.

(105) Rodriguez F, Langer F, Harrington KB et al. Alterations in transmural strains adjacent to ischemic myocardium during acute midcircumflex occlusion. *J Thorac Cardiovasc Surg* 2005 April;129(4):791-803.

(106) Salazar HP, Talano JV. Viable myocardium: how much is enough? *Echocardiography* 2005 January;22(1):59-70.

(107) Schmidt RF LFHM. Physiologie des Menschen. Mit Pathophysiologie. Springer-Verlag Heidelberg . 1-9-2007.

(108) Schmidt-Nielsen K, Duke JB. Animal Physiology Adaptation and Environment. Cambridge University Press . 1975.

(109) Selvanayagam JB, Kardos A, Francis JM et al. Value of delayed-enhancement cardiovascular magnetic resonance imaging in predicting myocardial viability after surgical revascularization. *Circulation* 2004 September 21;110(12):1535-41.

(110) Sengupta PP, Khandheria BK, Korinek J, Wang J, Belohlavek M. Biphasic tissue Doppler waveforms during isovolumic phases are associated with asynchronous deformation of subendocardial and subepicardial layers. *J Appl Physiol* 2005 September;99(3):1104-11.

(111) Sengupta PP, Krishnamoorthy VK, Korinek J et al. Left ventricular form and function revisited: applied translational science to cardiovascular ultrasound imaging. *J Am Soc Echocardiogr* 2007 May;20(5):539-51.

(112) Shivalkar B, Maes A, Borgers M et al. Only hibernating myocardium invariably shows early recovery after coronary revascularization. *Circulation* 1996 August 1;94(3):308-15.

(113) Sicari R, Nihoyannopoulos P, Evangelista A et al. Stress Echocardiography Expert Consensus Statement--Executive Summary: European Association of Echocardiography (EAE) (a registered branch of the ESC). *Eur Heart J* 2009 February;30(3):278-89.

(114) Sluysmans T, Colan SD. Theoretical and empirical derivation of cardiovascular allometric relationships in children. *J Appl Physiol* 2005 August;99(2):445-57.

(115) Steine K, Rossebo AB, Stugaard M, Pedersen TR. Left ventricular systolic and diastolic function in asymptomatic patients with moderate aortic stenosis. *Am J Cardiol* 2008 October 1;102(7):897-901.

(116) Stoylen A. Strain and strain rate imaging of the left ventricle by ultrasound. Feasibility, clinical validation and physiological aspects. Thesis, Norwegian University of Science and Technology Faculty of Medicine , 1-67. 2001.

(117) Stoylen A, Heimdal A, Bjornstad K, Torp HG, Skjaerpe T. Strain Rate Imaging by Ultrasound in the Diagnosis of Regional Dysfunction of the Left Ventricle. *Echocardiography* 1999 May;16(4):321-9.

(118) Stoylen A, Heimdal A, Bjornstad K et al. Strain rate imaging by ultrasonography in the diagnosis of coronary artery disease. *J Am Soc Echocardiogr* 2000 December;13(12):1053-64.

(119) Strobeck JE, Krueger J, Sonnenblick EH. Load and time considerations in the force-length relation of cardiac muscle. *Fed Proc* 1980 February;39(2):175-82.

(120) Strobeck JE, Sonnenblick EH. Myocardial and ventricular function. Part II: Intact heart. *Herz* 1981 October;6(5):275-87.

(121) Strotmann JM, Janerot-Sjoberg B, Kimme P et al. The effect of pacing-induced heart rate variation on longitudinal and circumferential regional myocardial function after acute beta-blockade--a cardiac ultrasound study. *Eur J Echocardiogr* 2000 September;1(3):184-95.

(122) Suarez dL, Casey P, Casey A et al. Effects of acute changes in load and inotropic state on the exponential rate of fiber shortening and other indices of myocardial contractility in the anesthetized intact dog. *Can J Physiol Pharmacol* 1987 January;65(1):46-53.

(123) Sutherland GR, Hatle L, Rademakers FE, Claus P, D`Hooge J, Bijnens B. Doppler Myocardial Imaging. A Textbook. 2004.

(124) Takayama M, Norris RM, Brown MA, Armiger LC, Rivers JT, White HD. Postsystolic shortening of acutely ischemic canine myocardium predicts early and late recovery of function after coronary artery reperfusion. *Circulation* 1988 October;78(4):994-1007.

(125) Takehana K, Ruiz M, Petruzella FD, Watson DD, Beller GA, Glover DK. Response to incremental doses of dobutamine early after reperfusion is predictive of the degree of myocardial salvage in dogs with experimental acute myocardial infarction. *J Am Coll Cardiol* 2000 June;35(7):1960-8.

(126) Theroux P, Franklin D, Ross J, Jr., Kemper WS. Regional myocardial function during acute coronary artery occlusion and its modification by pharmacologic agents in the dog. *Circ Res* 1974 December;35(6):896-908.

(127) Theroux P, Ross J, Jr., Franklin D, Kemper WS, Sasyama S. Regional Myocardial function in the conscious dog during acute coronary occlusion and responses to morphine, propranolol, nitroglycerin, and lidocaine. *Circulation* 1976 February;53(2):302-14.

(128) Underwood SR, Bax JJ, vom DJ et al. Imaging techniques for the assessment of myocardial hibernation. Report of a Study Group of the European Society of Cardiology. *Eur Heart J* 2004 May;25(10):815-36.

(129) Urheim S, Edvardsen T, Torp H, Angelsen B, Smiseth OA. Myocardial strain by Doppler echocardiography. Validation of a new method to quantify regional myocardial function. *Circulation* 2000 September 5;102(10):1158-64.

(130) Vatner SF. Correlation between acute reductions in myocardial blood flow and function in conscious dogs. *Circ Res* 1980 August;47(2):201-7.

(131) Vitarelli A, Montesano T, Gaudio C et al. Strain rate dobutamine echocardiography for prediction of recovery after revascularization in patients with ischemic left ventricular dysfunction. *J Card Fail* 2006 May;12(4):268-75.

(132) Wang J, Urheim S, Korinek J, Abraham TP, McMahon EM, Belohlavek M. Analysis of postsystolic myocardial thickening work in selective myocardial layers during progressive myocardial ischemia. *J Am Soc Echocardiogr* 2006 September;19(9):1102-11.

(133) Weidemann F, Herrmann S, Stork S et al. Impact of myocardial fibrosis in patients with symptomatic severe aortic stenosis. *Circulation* 2009 August 18;120(7):577-84.

(134) Weidemann F, Jamal F, Sutherland GR et al. Myocardial function defined by strain rate and strain during alterations in inotropic states and heart rate. *Am J Physiol Heart Circ Physiol* 2002 August;283(2):H792-H799.

(135) Weidemann F, Jung P, Hoyer C et al. Assessment of the contractile reserve in patients with intermediate coronary lesions: a strain rate imaging study validated by invasive myocardial fractional flow reserve. *Eur Heart J* 2007 June;28(12):1425-32.

(136) Weidemann F, Strotmann JM. Detection of subclinical LV dysfunction by tissue Doppler imaging. *Eur Heart J* 2006 August;27(15):1771-2.

(137) Weidemann F, Wacker C, Rauch A et al. Sequential changes of myocardial function during acute myocardial infarction, in the early and chronic phase after coronary intervention described by ultrasonic strain rate imaging. *J Am Soc Echocardiogr* 2006 July;19(7):839-47.

(138) Wyman BT, Hunter WC, Prinzen FW, McVeigh ER. Mapping propagation of mechanical activation in the paced heart with MRI tagging. *Am J Physiol* 1999 March;276(3 Pt 2):H881-H891.

(139) Yasuoka K, Harada K. Wall motion velocities of abdominal aorta measured by tissue Doppler imaging in normal children. *Pediatr Cardiol* 2005 July;26(4):323-7.

(140) Yildirim A, Soylu O, Dagdeviren B, Zor U, Tezel T. Correlation between Doppler derived dP/dt and left ventricular asynchrony in patients with dilated cardiomyopathy: A combined study using strain rate imaging and conventional Doppler echocardiography. *Echocardiography* 2007 May;24(5):508-14.

(141) Zeng S, Zhou QC, Peng QH et al. Assessment of regional myocardial function in patients with dilated cardiomyopathy by velocity vector imaging. *Echocardiography* 2009 February;26(2):163-70.

(142) Zhang Y, Chan AK, Yu CM et al. Strain rate imaging differentiates transmural from non-transmural myocardial infarction: a validation study using delayed-enhancement magnetic resonance imaging. *J Am Coll Cardiol* 2005 September 6;46(5):864-71.

12 Appendix Paper I-III